***Carnets Geol.* 26 (16)**

EISSN 16340744
DOI: 10.2110/carnets.2026.2616

Late Jurassic-Early Cretaceous phytoplankton ecosystem evolution interrupted by the late Valanginian WEISSERT carbon isotope event

Robert W. SCOTT [1]

Abstract: The Late Jurassic-Early Cretaceous Phytoplankton Ecosystem Evolution and its associated Calcification Event were major evolutionary innovations of calcareous marine pelagic micro-organisms. Beginning about 160 Ma in the Oxfordian Stage calcareous nannofossils and calcareous dinoflagellates began calcifying their tests that subsequently accumulated as calcareous ooze. By the Tithonian Stage and continuing into the early Valanginian, calpionellids added to the diversification and expansion of this new pelagic ecosystem. This gradual, progressive ecosystem change in the oceanic photic realm was associated with increased–burial of light carbon isotope. This calcareous plankton ecosystem suffered a crisis about 135 Ma by the late Valanginian Carbon Isotope Excursion. This isotope excursion was temporally related to emplacement of the Paraná-Etendeka LIP in the Paraná Basin in South America.

The upper Valanginian Carbon Isotope Excursion (VCIE) is a positive $\delta^{13}C$ peak 1.5‰ to 3.0‰. In a thick terrigenous section, Japan, this excursion has four subunits bracketed by three radioisotope ages on ash beds. The VCIE began at 135.56 Ma and ended at 132.50 Ma. Its mean duration was 2.47 Myr. The VCIE subunits are correlated globally. Among these sections the age of the VCIE spans from 135.79 Ma to 132.25 Ma.

The VCIE documents increased terrigenous sediment deposition and relative sea-level rise in the Gulf of Mexico, west-central Atlantic, France, Italy, and Oman. Globally, climate became more humid with lower atmospheric pCO_2 as subaerial volcanics were emplaced and weathered. Coincident was the late Valanginian Nannofossil-Calpionellid-Calcareous-Dinoflagellate Crisis characterized by decreased abundance and diversity of these three groups. The biotic crisis is related to the VCIE and changing paleoenvironmental processes. This study illustrates ocean-climate processes that affected the latest Jurassic-earliest Cretaceous Earth system.

Keywords:

- phytoplankton evolution;
- Tithonian-Berriasian calcification event;
- Valanginian biotic crisis;
- Valanginian WEISSERT Excursion;
- Valanginian excursion subunits;
- age of Valanginian chemozone

Citation: SCOTT R.W. (2026).- Late Jurassic-Early Cretaceous phytoplankton ecosystem evolution interrupted by the late Valanginian WEISSERT carbon isotope event.- *Carnets Geol.*, Madrid, vol. 26, no. 16, p. 355-375. DOI: 10.2110/carnets.2026.2616

Résumé : *Évolution de l'écosystème phytoplanctonique du Jurassique supérieur au Crétacé inférieur, interrompue par l'événement isotopique (δ13C) WEISSERT au Valanginien supérieur.-* L'évolution de l'écosystème phytoplanctonique du Jurassique supérieur au Crétacé inférieur, ainsi que l'événement de calcification qui lui est associé, constituent des innovations évolutives majeures chez les microorganismes marins pélagiques calcaires. À partir d'environ 160 Ma, au cours de l'Oxfordien, les nannofossiles calcaires et les dinoflagellés calcaires ont commencé à calcifier ; ces microstructures se sont ensuite accumulées sous forme de boues calcaires. En outre, à partir du Tithonien et jusqu'au début du Valanginien, les calpionelles ont également contribué à la diversification et à l'expansion de ce nouvel écosystème pélagique. Cette évolution progressive et graduelle de l'écosystème dans la zone photique océanique s'est accompagnée d'un enfouissement accru de l'isotope léger du carbone. Cet écosystème de plancton calcaire a subi une crise vers 135 Ma, lors de l'excursion isotopique (δ13C) du Valanginien supérieur. Cette excursion isotopique a été contemporaine de la mise en place de la grande province magmatique du Paraná-Etendeka dans le bassin du Paraná, en Amérique du Sud.

[1] Precision Stratigraphy Associates, 140 East 21st Street, Tulsa, Oklahoma 74114 (U.S.A.)
rwscott971@gmail.com

Published online in final form (pdf) on September xx, 2026
[Editor: Bruno R.C. GRANIER]

L'excursion isotopique (δ13C) du Valanginien supérieur (VCIE, *Valanginian Carbon Isotope Excursion*) correspond à un pic positif de $\delta^{13}C$ compris entre 1,5 ‰ et 3,0 ‰. Dans une épaisse série terrigène du Japon, cette excursion comprend quatre sous-unités, encadrées par trois datations radio-isotopiques réalisées sur des niveaux de cendres volcaniques. La VCIE a débuté à 135,56 Ma et s'est achevée à 132,50 Ma pour une durée moyenne de 2,47 millions d'années. Les sous-unités de la VCIE sont corrélées à l'échelle mondiale. Dans les différentes séries étudiées, l'âge de la VCIE s'étend de 135,79 Ma à 132,25 Ma.

La VCIE témoigne d'une augmentation des dépôts de sédiments terrigènes ainsi que d'une élévation relative du niveau marin dans le golfe du Mexique, l'Atlantique occidental et central, en France, en Italie et en Oman. À l'échelle mondiale, le climat est devenu plus humide, avec une diminution du pCO_2 atmosphérique, tandis que des roches volcaniques se mettaient en place en domaine émergé puis étaient soumises à l'altération. Cette période coïncide avec la crise des nannofossiles calcaires, des calpionelles et des dinoflagellés calcaires du Valanginien supérieur, caractérisée par une diminution de l'abondance et de la diversité de ces trois groupes. Cette crise biologique est liée à la VCIE et aux modifications des processus paléoenvironnementaux. Cette étude illustre les processus océaniques et climatiques qui ont affecté le système Terre dans l'intervalle Jurassique terminal - Crétacé basal.

Mots-clefs :

- évolution du phytoplancton ;
- événement de calcification du Tithonien-Berriasien ;
- crise biotique du Valanginien ;
- excursion isotopique WEISSERT du Valanginien ;
- sous-unités de l'excursion du Valanginien ;
- âge de la chémozone du Valanginien

1. Introduction

The Late Jurassic-Early Cretaceous oceans experienced the onset of calcification of major pelagic microbiota. This change drastically altered the marine planktonic paleocommunity and initiated deposition of marine calcareous ooze. Calcareous nannoplankton, calcareous dinoflagellates and calpionellid loricas became widespread and common organisms in the pelagic zone and were deposited as deep-sea ooze becoming limestone and marl. Consequently, these fossil groups are now important biostratigraphic markers of Tithonian, Berriasian and Valanginian stages. The acme of these groups, however, was stunted in late Valanginian by a significant increase in $\delta^{13}C$ ‰ and changes in sea-surface temperature and partial CO_2 pressure, and possibly increased trace element concentrations including phosphorus. This event has been identified as the WEISSERT Valanginian Carbon Isotope Excursion Excursion (VCIE) (ERBA & TREMOLADA, 2004).

Chemozones, such as the Valanginian CIE, are integral to stratigraphic correlation and interpretation of paleoceanography and paleoclimates (SCOTT *et al.*, 2023). The earliest Early Cretaceous positive carbon isotope excursion in bulk carbonate and organic matter was initially identified in marine facies in Italy and France (reviewed by WEISSERT *et al.*, 2008). The upper Valanginian Carbon Isotope Excursion (VCIE) was documented in pelagic limestone of the Maiolica Formation deposited along the northern Tethys margin now in northern Italy (WEISSERT *et al.*, 1985; ERBA *et al.*, 2015). Initially this $\delta^{13}C$ excursion was viewed as a rather symmetrical positive peak from 1.5‰ to 3.0‰ spanning the upper Valanginian substage and locally extending into the lowermost Hauterivian Stage as defined by calcareous nannofossils (LINI *et al.*, 2007; WEISSERT *et al.*, 2008). Subsequent interpreters placed boundaries at different points on the curve, such as the inflection points where the isotope values increase or decrease or at the peaks. Boundaries were also placed at the peak where the isotope values begin to decrease or where they flatten out (HENNIG FISCHER, 2003) resulting in different correlation and timing results.

The Valanginian carbon isotope excursion is reported globally in the Tethys Realm as well as in the Boreal Arctic and Southern Antarctic regions (GRÉSELLE *et al.*, 2011; MÖLLER *et al.*, 2015; ALLEY *et al.*, 2020; CHARBONNIER *et al.*, 2020; JELBY *et al.*, 2020; CAVALHEIRO *et al.*, 2021). It is recorded in shallow-water carbonate facies, deep water facies, lacustrine facies (TONG *et al.*, 2024), and in pedogenic terrestrial facies (JOECKEL *et al.*, 2023). Here, the denomination of this excursion is simplified to Valanginian Carbon Isotope Excursion (VCIE) so that its name is consistent with names of younger Cretaceous carbon isotope excursions.

This study correlates the VCIE based upon lithostratigraphic, biostratigraphic and chemostratigraphic data from deep-sea cores collected during the past fifty years. Consequently, data quality varies because collection and processing standards have evolved. In most sections bulk limestone samples were processed for $\delta^{13}C$ and in a few sections organic matter was processed, but no attempt was made to determine the sources of the organic matter that produced the isotopes as is now required (SUAN *et al*., 2015; BODIN *et al*., 2023). Also the fractionation between organic matter and carbonate was not considered (HAYES *et al.*, 1999). Nevertheless, the four-fold pattern of the VCIE identified in the Japanese Koyamada Formation (TOMARU *et al.*, 2025) will be tested to determine whether it represents–a global signal that can be identified in older carbon isotope curves. Recent research is subdividing the carbon isotope curve at basal and upper peaks (CAVALHEIRO *et al.*, 2021).

Another issue is correlation of the VCIE with the Cretaceous time scale and the recently agreed upon Valanginian GSSP. In many sections the VCIE spans the upper Valanginian (Bottini *et al.*, 2018; Cavalheiro *et al.*, 2021), but in the Pont de Carajuan section the onset stage is reported in the lower Valanginian (Hennig *et al.*, 1999; Martinez *et al.*, 2015). In this section the onset began in the *Busnardoites campylotoxus* Subzone of the lower Valanginian *Neocomites neocomiensiformis* Zone and the highest peak was in the upper Valanginian *Neocomites peregrinus* Zone.

To address this issue, a biostratigraphic database was constructed from 124 measured outcrops and cored sections, the Cretaceous 25 Chronostratigraphic Database (CRET25DB). This database includes the Valanginian GSSP Montbrun-les-Bains and the Hauterivian La Charce GSSP sections. Check-lists of these localities document First-Occurrences and Last-Occurrences (FO/LO) of events in given sections. These events were integrated into a global chronostratigraphic database, CRET25DB, that integrates FOs/LOs as First-Appearance Datums and Last-Appearance Datums (FAD/LAD) in multiple sections. This database evolved from previous Cretaceous databases (Scott, 2019, 2022). It incorporates radioisotopic dates, sequence contacts and polarity chrons where available. This Cretaceous databasewas used to correlate eight marine stratigraphic sections with carbon isotope profiles in outcrops and cores from the Western Atlantic, Vocontian Basin, Arabian shelf, Japan, and Weddell Sea and in two terrestrial sections in North America and China (Fig. 1; Table 1)

The primary goal of this study is to integrate global biotic events of Tithonian-Valanginian nannofossils, dinoflagellates and calpionellids with the Valanginian Carbon Isotope Excursion and to consider their effects upon the pelagic paleocommunities. To achieve this goal, evidence of the calcification process of three principal fossil groups is synthesized. Second, the numerical ages of boundaries of the Valanginian Carbon Excursion and its subunits are calibrated in the Koyamada Formation, Japan. The ages of subunits in the Koyamada Formation are projected from three radioisotope dates of volcanic material in the composited outcrop sections (Tomaru *et al.*, 2025). A third goal is to define the boundaries of the VCIE precisely and consistently, in order to correlate the VCIE and its subunits in other sections. Precise definition of this chemozone enables accurate chemostratigraphic correlation of the excursion and reconstruction of paleo-oceanic and paleoclimatic conditions during this paleoenvironmental perturbation. The precise correlation of the VCIE demonstrates that this excursion is a global chemozone with multiple peaks and it has global paleoenvironmental implications affecting evolution of the global marine pelagic ecosystem.

2. Methods: Construction of CRET25DB

The Cretaceous Chronostratigraphic Database (CRET25DB) is composed of the first and last appearances of more than 2,800 stratigraphic items: species, polarity chrons, dated bentonite and ash beds, and other types of marker beds. The ranges of these events were integrated by graphic correlation of check-lists and range charts in 124 measured outcrop sections and cores in North, Central and South America, Europe, Africa, Asia, and Japan (Fig. 1). Also included are the accepted or proposed Cretaceous stage Global Boundary Stratotype Sections and Points (GSSPs) and the species that define their boundaries. The CRET25DB grew out of previous databases (Scott, 2019, 2022).

The method used to perform this stratigraphic experiment is Graphic Correlation, which is a transparent, reproducible, testable method that integrates biostratigraphic First/Last Occurrences (FOs/LOs) and other chronostratigraphic events in multiple measured sections (Carney & Pierce, 1995). Graphic correlation is a quantitative but non-statistical technique that enables stratigraphic correlation between two sections by comparing the ranges of event records in both sections. A graph of any pair of sections is an X/Y plot of the FOs/LOs of taxa and other types of stratigraphic datums found in both the section of interest (Y-axis) and the reference section (X-axis). To propose coeval relationships between sections, the interpreters place a correlation line of synchroneity (CLS) through the FOs/LOs that are at their maximum ranges in both sections. This CLS is the most constrained hypothesis of synchroneity between two sections and extends the ranges of the fewest bioevents onto the CLS. The CLS accounts for depositional rate changes, hiatuses, differential mechanical and chemical compaction, and tectonic processes. Hiatuses at stratal discontinuities or faults in the lithostratigraphic record divide the CLS into separate segments. The CLS is defined by the equation for a regression line (Carney & Pierce, 1995). The integrated ranges of the initial pair of sections form a reference section to which subsequent sections are plotted and the ranges in the new sections are then extended to comprise a composite set of ranges. Biostratigraphic ranges were integrated in multiple sections and extended FADs/LADs. Graphic correlation was used to integrate shallow-water carbonate platform fossils with deep marine assemblages spanning from Oxfordian to Hauterivian interval (Atasoy *et al.*, 2022).

The CRET25DB biostratigraphic ranges are calibrated to the mega-annum time scale of Gale *et al.* (2020) by incorporating radioisotopic dates into the combined data set. Published radioisotope dates include the three dates from the Koyamada Formation. The accuracy of fossil-age ranges depends on the number of sections in

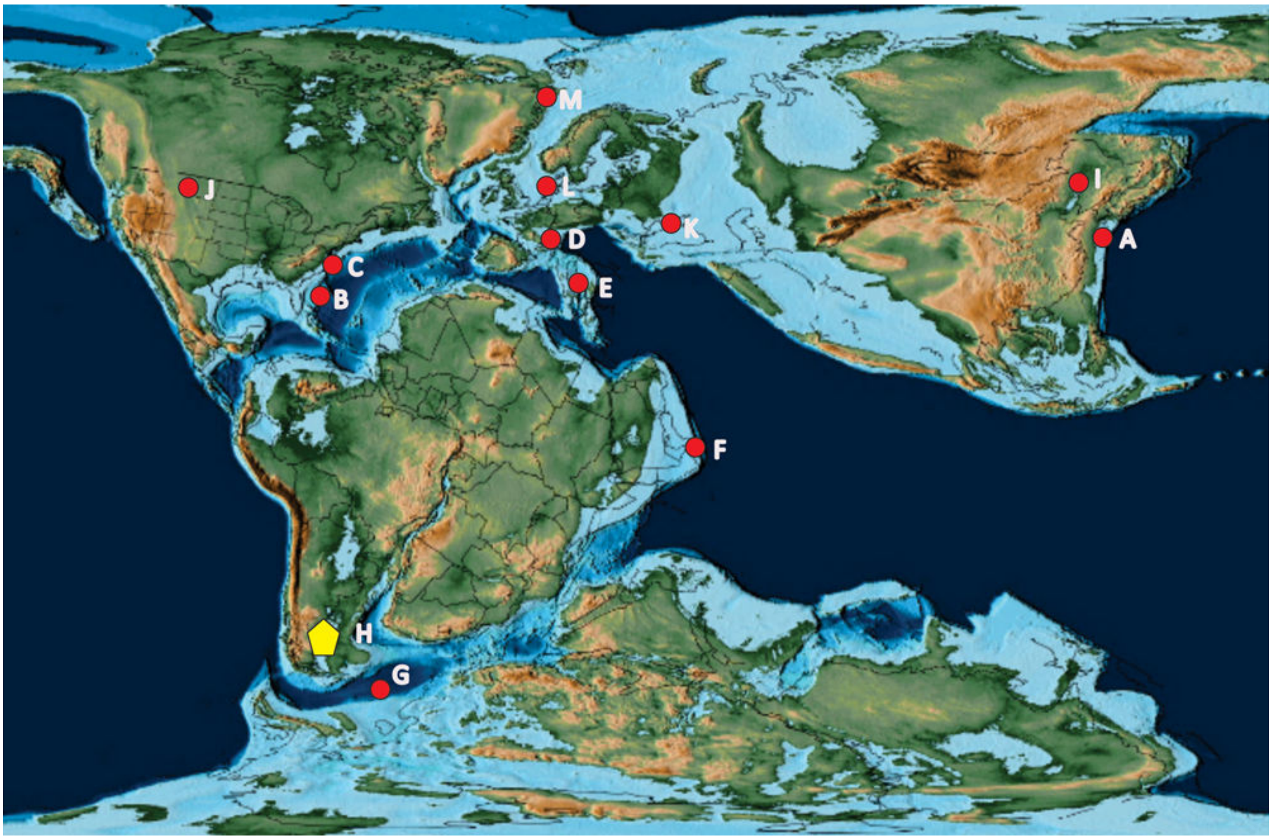

Figure 1: Hauterivian paleogeographic map (Scotese, 2013) showing sites of this study. **A.** Koyamada Formation, Japan (Tomaru *et al.*, 2025); **B.** DSDP 534A (Sheridan, 1983; Bergen, 1994); **C.** DSDP 603B (Covington & Wise, 1987; Habib & Drugg, 1987); **D.** Vocontian Basin, France: La Charce (Grésel le *et al.*, 2011); Orpierre (Charbonnier *et al.*, 2013); Pont de Carajuan (Arnaud & Bulot, 1992); **E.** Capriolo, Italy (Hennig *et al.*, 1999); **F.** Wadi Miadin, Oman (Celestino *et al.*, 2016); **G.** ODP 692B (Cavalheiro *et al.*, 2021); **H.** Paraná-Etendeka LIP (Tomaru *et al.*, 2025); **I.** Luanping Basin, China (Tong *et al.*, 2024); **J.** Utahraptor Ridge, Montana (Joeckle *et al.*, 2023); **K.** Crimea (Gröcke *et al.*, 2005); **L.** Lower Saxony Basin (Thöle *et al.*, 2020); **M.** Svalbard (Jelby *et al.*, 2020).

which the events are recorded, fossil preservation, correct identification of the species, and recognition of reworking or down-section displacement of specimens. Event sequences and ages compiled by graphic correlation can be tested and fully evaluated because the sources of the data are available to all researchers. This experimental method complements and is tested by the prevalent practice of the corporate memory of events in many sections. In addition, the order of events in different basins and paleogeographic provinces can be compared.

Fourteen localities were selected in which biostratigraphic, lithostratigraphic, magnetostratigraphic, and chemostratigraphic data of the VCIE are well documented (Fig. 1). These sections span from northern to southern latitudes and biogeographic provinces. They represent diverse marine and terrestrial paleoenvironments. Biostratigraphic data include range charts of multiple fossil groups in checklist form. The first and last occurrences (FO/LO) of each species in each section were compiled into data files for each section. Added to each section file were positions of unconformities, faults, polarity chrons, and geochemical data. The range data of each section was plotted on the Y-axis and compared to the numerically dated CRET25DB on the X-axis and the CLS was interpreted.

The plot of the west-central Atlantic DSDP 603B core with the CRET25DB illustrates this technique (Fig. 2). Base of the plot is the base of the core and the top is a condensed interval between -1215 and -1205.5 mbsf. The interpreted CLS is controlled by the base of the Onset interval in VCIE, which is close to the FO of *Kiokansium polypes* and the LO of *Spiniferites dentatus* (Fig. 2). The CLS falls slightly left of the highest position of VCIE and does not extend it.

3. Late Jurassic-Early Cretaceous phytoplankton ecosystem evolution

During the twenty-five Myr interval from the Oxfordian Stage to early Valanginian, the pelagic ecozone became progressively populated by diverse and abundant calcareous coccolithophore and dinoflagellate phytoplankton (Price *et al.*, 2016), here called the Late Jurassic-Early Cretaceous Phytoplankton Ecosystem Evolution. This was the beginning of the Mesozoic Marine Revolution (MMR) (Vermeij, 1977; Hull, 2017), which gave rise to the Late Cretaceous, Cenozoic and Holocene ocean ecosystems. The dinoflagellates

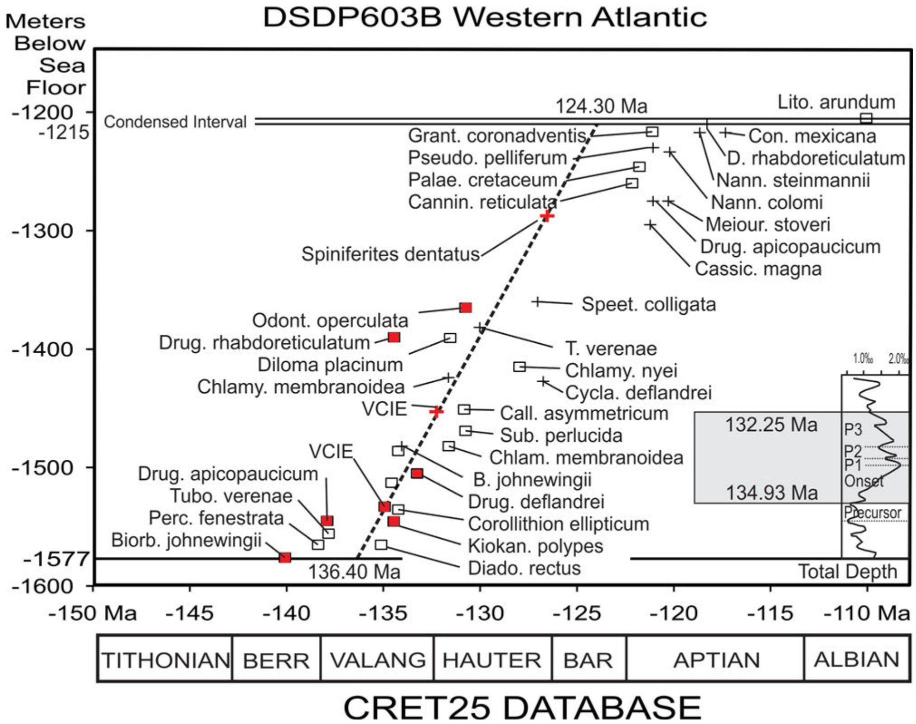

◀ **Figure 2:** Correlation of lower part of DSDP-603B core with the CRET25 Database. Base of the plot is core base and plot top is a condensed interval, core subunit IVD; data from Covington and Wise (1987) and Habib and Drugg (1987). The CLS is constrained by the FOs (rectangles) and LOs (crosses) of zone species (red). The VCIE curve is projected into the CLS showing the positions of the base and top of the chemozone.

first began diversifying in Middle Jurassic (Wiggan *et al.*, 2018). The Oxfordian-Valanginian phytoplankton radiation responded to increased nutrients, which during the later part of the Cretaceous provided primary production that prompted radiation in many other marine groups (Knoll & Follows, 2016). The Late Jurassic to Early Cretaceous ecosystem radiation phase also affected crabs, echinoids and heteromorph ammonoids (Fraaije *et al.*, 2018). During the Oxfordian-early Valanginian ocean parameters were relatively stabile and changed unidirectionally. Sea level rose from Oxfordian to Kimmeridgian, fell during the Tithonian, rose in the Berriasian, and fell in the early part of the Valanginian and then rose during the VCIE (Fig. 3) (Ray *et al.*, 2019; Falkowski *et al.*, 2004; Scotese *et al.*, 2024). The magnitude of short-term sea-level changes were low amplitude in the Berriasian even as Gondwana began to disengage and increased up to three times in the Valanginian (Fig. 3) (Ray *et al.*, 2019). Belemnite oxygen isotopes show that global ocean temperature changes were moderate until late Berriasian (Price *et al.*, 2016). The secular trend towards lower $\delta^{13}C$ values was interrupted abruptly in the late Valanginian at 135 Ma when burial of light carbon isotope increased that resulted in the positive VCIE. During this period of open-ocean climate stability, calcareous coccolith and dinoflagellate phytoplankton diversified and contributed significant amount of $CaCO_3$ to sea-floor sediment. Calpionellid plankton formed calcite tests in the Tithonian Stage and were abundant until their virtual extinction near the Valanginian-Hauterivian boundary (Fig. 3). The increased diversification and abundance of these three pelagic groups formed the Late Jurassic-Early Cretaceous Phytoplankton Ecosystem. Calcareous planktonic foraminifera appeared in Early Jurassic but did not diversify until the Aptian Stage (Hart *et al.*, 2002; Gradstein *et al.*, 2017). Because they are uncommon in open ocean Jurassic paleocommunities, they are not considered here.

Tithonian-Berriasian calcification event

Calcareous pelagic and benthic marine biota became the characteristic ecosystem members beginning in Tithonian to early Valanginian. The latest Jurassic-earliest Cretaceous Calcification Event (Cavalheiro *et al.*, 2021) recognizes the increase of calcareous nannofossils, calpionellids, and calcareous and organic-walled dinoflagellate cysts. Planktonic microbiota precipitated calcareous tests around their protoplasm that was deposited as calcareous ooze.

The oldest known calcareous nannofossils are Late Triassic (Bown *et al.*, 1998). Throughout the Jurassic and Early Cretaceous nannofossils diversified continuously with peaks around the Toarcian and Valanginian OAEs (Bown *et al.*, 2004: Fig. 2). Speciation and extinction rates were highest in Early Jurassic up to the Toarcian Stage, when seawater temperature increased by at least 10°C up to 25-30°C before cooling back to about 10°C (Korte *et al.*, 2015). Spanning the Tithonian and Berriasian stages the nannofossil assemblages experienced significant turnover with extinctions and originations of three important groups: nannoconids, braarudosphaerids and microrhabdulids (Fig. 4) (Bown *et al.*, 2004). Nannoconids dominated Berriasian-Valanginian pelagic sediments replacing radiolarians. Although, during the VCIE event, nannofossil diversity increased, the calcite accumulation was low (Fig. 4).

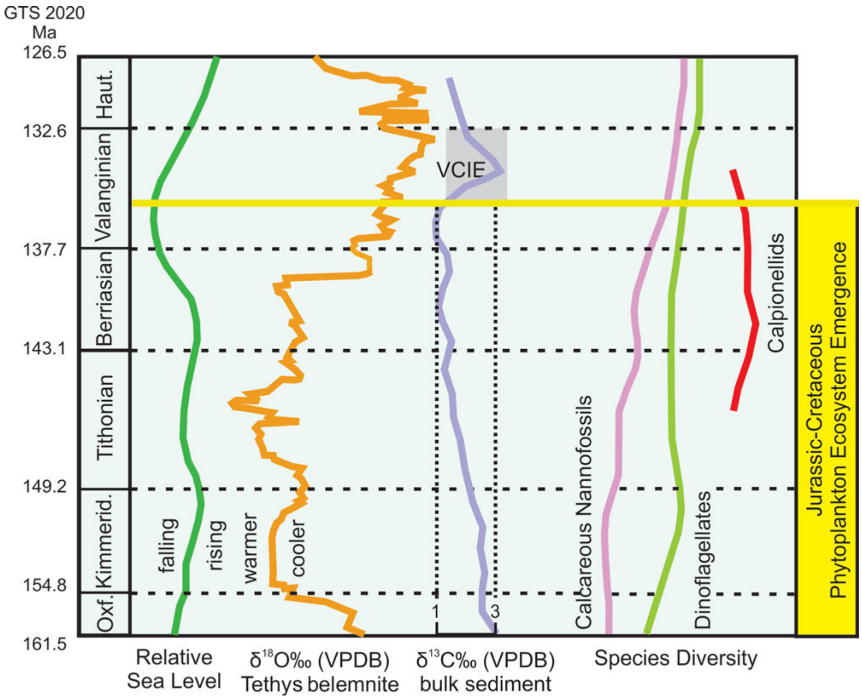

◀ **Figure 3:** Late Jurassic-Early Cretaceous Phytoplankton Diversification Evolution. Relative sea-level and diversity curves of calcareous nannoplankton and dinoflagellates from FALKOWSKI *et al.* (2004); oxygen isotope and carbon isotope curves from PRICE *et al.* (2016).

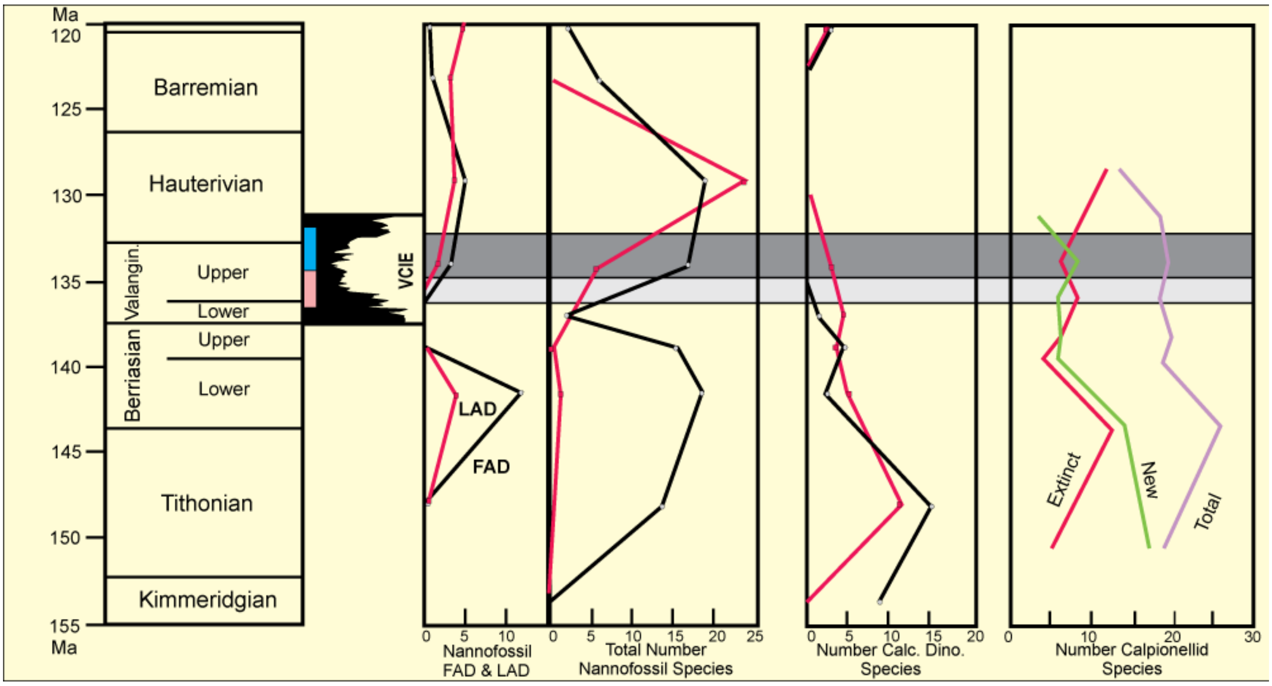

Figure 4: Number of nannofossil, dinoflagellate and calpionellid species in the CRET25 Database. The range of the VCIE event is represented by diversity data in the Polaveno core. Warm and cool intervals marked by pink and blue bars. Number of species extinctions indicated by LAD curve and number of new species by FAD. Total number of calpionellid species (blue), number of new species (green) and number of extinct species (red) in ammonite zones based on range data in CRET25 Database.

Calcareous dinoflagellates, such as *Colomiosphaera* and *Cadosina*, diversified in early Tithonian in the southern oceans and became extinct by the end of the Berriasian (IVANOVA & KIETZMANN, 2017). In shallow-water shelves rudist bivalves first formed thick-walled aragonite shells in Oxfordian biostromes and diversified into the Tithonian (STEUBER *et al.*, 2016). Sea level rose across the globe (COTILLON, 1992; HAQ, 2014) and deeper water shelf-to-basin habitats expanded. Earlier Jurassic carbonate habitats were drowned and fine-grained siliciclastic deposits expanded (COTILLON, 1992).

During this Calcification Event (CAVALHEIRO *et al.*, 2021) Chitinodellids and their descendent Calpionellids evolved complex wall structure in response to sea-water chemistry changes. Tithonian Chitinodellid diversification preceded the Calpionellid appearance in latest Tithonian (BENZAGGAGH, 2021), which expanded in the Berriasian and early Valanginian, after which calpionellids became nearly extinct (Fig. 5).

Calpionellidae is a diverse set of small, marine, pelagic ciliate microorganisms with calcitic, cylindrical to globular tests or loricas. Beginning in the Tithonian, calpionellids diversified rapidly and by early Berriasian the major groups were present (Fig. 4). Many taxa are characterized by distinctive collars around the lorica apertures (REHÁKOVÁ & MICHALÍK, 1997). Complex wall structure differentiated Calpionellids taxonomically. The ancestor calpionellid group, the Tithonian Chitinodellids, secreted dark microgranular calcite loricas (REHÁKOVÁ & MICHALÍK, 1997).

The earliest Tithonian Chitinodellids precipitated densely-packed, nanometric microcrystalline calcite needles to form the lorica wall (BENZAGGAGH, 2021; ÖLVECZKÁ *et al.*, 2024). Their descendants, the *Semichitinoidella*, followed in late Tithonian and formed a two-layered wall, the inner layer of which was microcrystalline calcite like that of *Chitinodella*. The outer layer was composed of prismatic microcrystalline, hyaline calcite crystals. The late Tithonian *Praetintinnopsella* formed a different two-layer wall, an inner hyaline layer of densely-packed equant calcite microcrystals and an outer dark organic non-calcitic layer. The earliest calpionellids, *Crassicolaria*, *Calpionella* and *Tintinnopsella*, formed hyaline tests (ÖLVECZKÁ *et al.*, 2024) (Fig. 5). The different ways in which to precipitate calcite wall structures suggests that significant changes occurred in mid-latitude ocean chemistry, possibly increased concentrations of Ca^{2+} and CO_2 as well as ocean warming.

Valanginian biotic crisis

The Valanginian Biotic Crisis beginning about 136-135 Ma affected most major marine pelagic groups (Figs. 4-5) (ERBA & TREMOLADA, 2004). This crisis began about one million years before the VICE and continued into it (Fig. 4). Calcareous nannofossils and nannoconids decreased in size, diversity and abundance (ERBA & TREMOLADA, 2004; CASELLATO *et al.*, 2008; MÖLLER *et al.*, 2015, 2020; BOTTINI *et al.*, 2018; CASELLATO & ERBA, 2021). This significant reduction in nannofossil calcification was related to decreased pCO_2 and increased fertility (ERBA & TREMOLADA, 2004). The calcification crisis began as sea-surface temperatures warmed (Fig. 6) (CAVALHEIRO *et al.*, 2021). The biotic change and positive carbon isotope shift are in dominantly terrigenous-rich intervals indicating increased terrigenous deposition in response to increased humidity and erosion (BOTTINI *et al.*, 2018).

Pelagic Calpionellid diversity declined significantly amplifying this crisis event (Figs. 4, 6). The organic-walled dinoflagellates, however, appeared to be barely affected by the Valanginian calpionellid-nannofossil crisis (MACRAE *et al.*, 1996; RIDING *et al.*, 2023). The Kimmeridgian dinoflagellate diversity peak was followed by a slight decline in the Berriasian (Fig. 4). However, a detailed analysis of 136 dinoflagellate taxa in CRET25DB having FADs between 150 Ma and 110 Ma, revealed that species diversification decreased significantly. Between 150 Ma and 135 Ma, 27.2% of species were new, but during the VCIE between 135 Ma and 131 Ma only 8.8% of species first appeared. Diversification resumed during the next 10 Myr with 21.3% new species. Planktonic foraminifera were minor members of the Late Jurassic-Early Cretaceous pelagic ecosystem, until the Barremian when their abundance and diversity slowly increased (AGUADO *et al.*, 2014).

By the late Valanginian in the *Neocomites peregrinus* Zone during the beginning of the VCIE, many Calpionellid species became extinct (Fig. 6) (REHÁKOVÁ & MICHALÍK, 1997), and at the Valanginian-Hauterivian transition they were virtually extinct (REMANE, 1985; ANDREINI *et al.*, 2007; LIPPS *et al.*, 2013; GRANIER *et al.*, 2024). They diversified again in the late Aptian and early Albian. By Barremian time the new Praecolomiellids appeared with micrograngular hyaline loricas. They were ancestors of the latest Aptian-early Albian Colomiellids with hyaline tests. They went extinct at the end of the early Albian after surviving the latest Aptian-early Albian OAE 1b chemozone.

Benthic ecosystems were also affected by the dramatic latest Jurassic-earliest Cretaceous Calcification Crisis and paleoclimate-paleoceanographic changes. The Oxfordian primitive rudist bivalves constructed low diversity biostromes on shallow-water shelves. They formed thick-walled aragonitic shells and diversified into the Kimmeridgian and Tithonian when some species secreted two-layered shells of both aragonite and calcite (STEUBER *et al.*, 2016: Fig. 7; 2023). Rudists experienced significant extinction at end of early Valanginian as the positive carbon excursion began. During the Hauterivian recovery, new species groups developed the ability to produce calcite-dominated shells. Rudists with aragonite-dominant shells diversified into the early Aptian when a second extinction occurred at the beginning of OAE 1a (STEUBER *et al.*, 2016: Fig. 6). These late Valanginian pelagic and benthic biota were associated with increased terrestrial erosion, clay influx, ocean fertilization and global cooling during the main parts of the VCIE (BORNEMANN & MUTTERLOSE, 2008; PERCIVAL *et al.*, 2023).

Berriasian-Hauterivian, deep-shelf brachiopod paleocommunities in central Tethys, now exposed in the Bakony Mountains, Hungary, experienced step-wise extinction (VÖRÖS *et al.*, 2020). During the transition from early to late Berriasian the first species replacement happened. The second step was at end of Berriasian into the Valanginian. Then, during the beginning of the Valanginian Carbon Isotope Excursion, eight species went extinct; of the two survivors, one was dwarfed. During latest Valanginian and into the Hauterivian, the recovery paleocommunity was populated by species apparently adapted to cooler waters. The recovery period was associated with rising sea level and increased weathering, which increased siliciclastic sediments (VÖRÖS *et al.*, 2020).

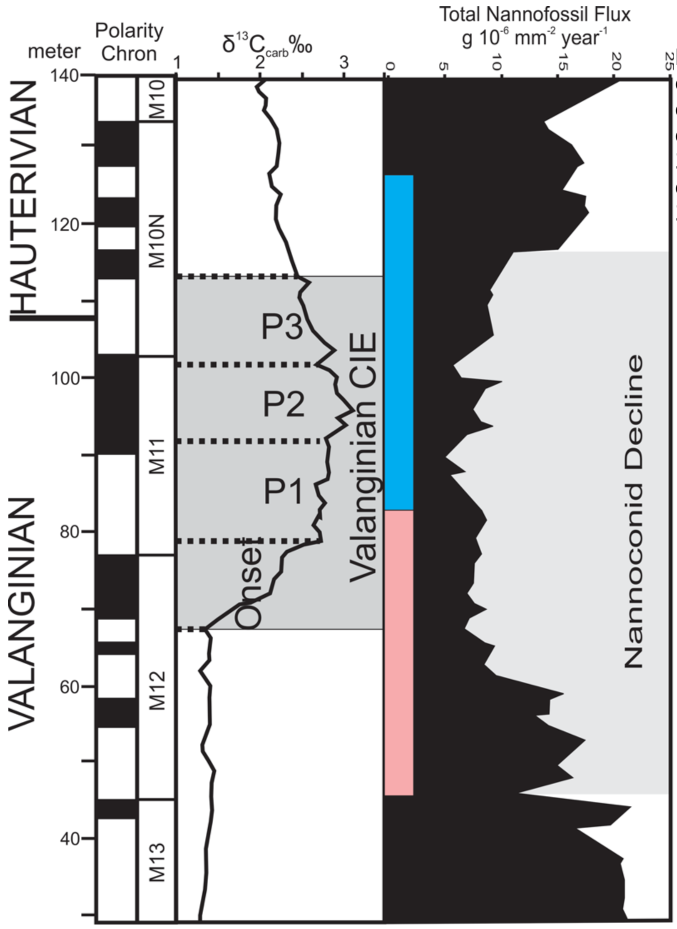

◀ **Figure 6:** Poloveno outcrop section, Italy, pelagic carbonate stratigraphy, polarity chrons, and carbon isotope curve plotted with total nannofossil carbonate paleoflux demonstrating nannoconid decline (CHANNEL *et al.*, 1995; ERBA & TREMOLADA, 2004) correlated with warm-cool temperature changes (rose & blue bars) (CAVALHEIRO *et al.*, 2021).

4. Subdivision and correlation of the Valanginian carbon isotope excursion

Numerical ages of VCIE subunits. TOMARU *et al.* (2025) divided the Valanginian Carbon Isotope Excursion (VCIE) into six elements in a 300 m-thick, organic-rich, siliciclastic interval along the east coast of Japan (Fig. 7). A composite stratigraphic section of the Koyamada Formation was composed of four measured, overlapping outcrops along a fault zone. Sample spacing in the excursion interval was about 0.5 m. Details of the $\delta^{13}C$ curve measured on organic matter are clearly delineated because the lithostratigraphic siliciclastic interval is much thicker than in thinner basinal sections (Fig. 7). In addition, three volcanic tuff beds yielded U-Pb zircon dates that bracket base to top of the excursion (TOMARU *et al.*, 2025: Fig. 8). The Koyamada Formation was sourced mainly by continental sediments deposited in an oxygenated marine environment with occasional brief dysoxic events based on analyses of total organic carbon (TOC), degree of pyritization (DOP) and total sulfur (TS) (TOMARU *et al.*, 2025). Yet to be determined are the admixture types of continental organic matter, as for example, in OAE 1b (SUAN *et al.*, 2015; BODIN *et al.*, 2023).

In order to interpolate numerical ages of the four subdivisions of the VCIE in the Koyamada Formation, Onset, P1, P2, and P3 subunits, the metric positions of these subunits were plotted to mega-annums of the three radioisotope dates measured in this outcrop (Fig. 7). This procedure created an approximate time scale and duration of the subunits. Also, if in other sections the isotope curve features vary, the placement of subunit boundaries may differ from those in the Japanese composite section. These numerical ages are compared with ages of ammonites, nannofossils, dinoflagellates, and polarity chrons in the global CRET25DB. This experiment dates the VCIE in the Koyamada Formation from 135.40 to 132.57 Ma, which is older than a start date of 134.56 ± 0.19 Ma calibrated by astrochonologic framework (MARTINEZ *et al.*, 2023).

Characteristics of the VCIE. The four subdivisions of the Valanginian carbon isotope curve can be defined consistently at either strong positive or negative peaks (TOMARU *et al.*, 2025) (Fig. 7). The basal subunit of the VCIE, noted as "CIE" by Tomaru and here called "Onset", is placed at the base of a narrow, distinct positive peak of about 1‰ at 80 m in the Koyamada Formation, which is at the base of the rise in isotope values to the first tall peak at 100 m, which is about 1.5‰ above the background value (Fig. 7) called "P1" (TOMARU *et al.*, 2025). Below this Onset interval is a span between two shallow negative peaks, which TOMARU *et al.* (2025) called the "Precursor". This preceding interval is highly variable and indistinct in other sections, so here the base of the VCIE is placed at the base of the Onset interval.

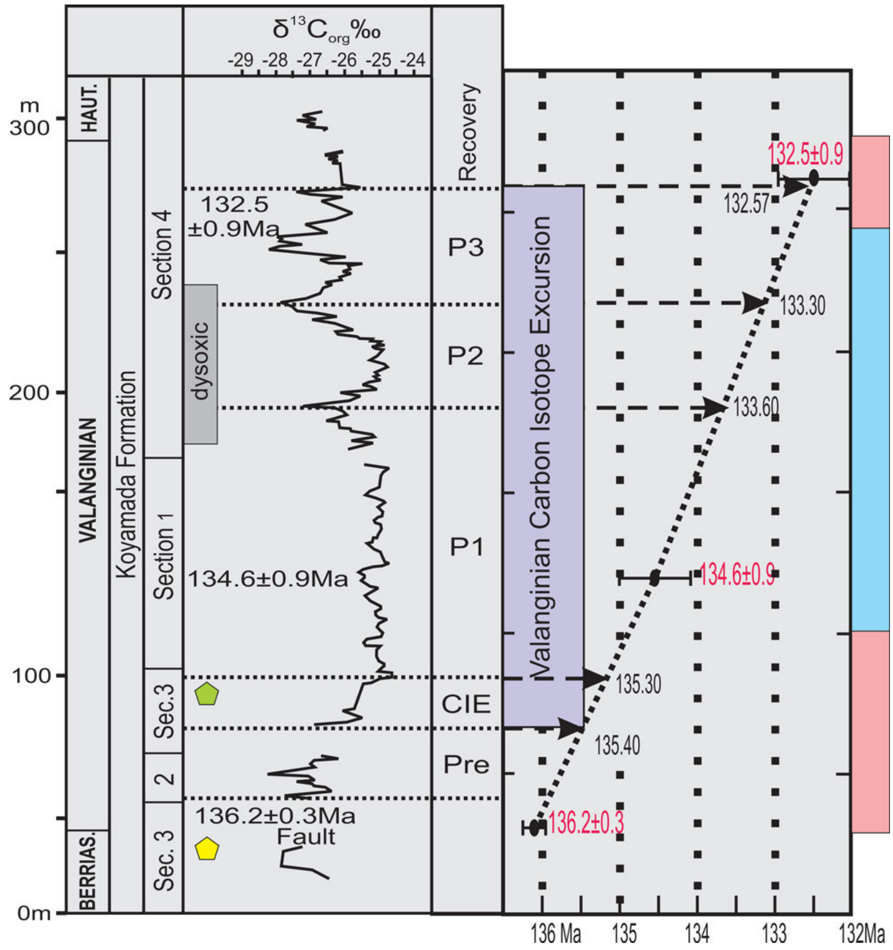

Figure 7: Projection of three radioisotope dates of ash beds (red) in the Koyamada Formation (TOMARU *et al.*, 2024) and calibration of ages of Valanginian CIE (gray bar) chemozone subunits. Yellow symbol - four Berriasian ammonite genera; green symbol - four Valanginian radiolarian taxa. Right-hand bar depicts warm (rose) and cool (blue) climates.

The P1 interval is thick and bounded at top at 195 m by a sharp negative shift about 1.0‰ or more (Fig. 7). The P2 interval is a narrow positive peak bounded at 230 m by a distinct, sharp negative offset. The P3 interval is broad spanning two positive peaks and it is bounded by a distinct negative shift at 275 m overlain by a long gentle slope to the background carbon isotope levels (Fig. 7). This negative peak is taken as the top of the VCIE. The "Recovery" part of the curve declines about 1‰ up to an unconformity. Because its character is indistinct in other stratigraphic sections, it is not included in the definition of VCIE. P3 is narrow in some sections.

The amplitudes of these shifts appear to be significantly above background of $\delta^{13}C$ fractionation, which at 133 Ma carbonate fractionation was about 1.5‰ and for TOC it was about -27‰, both of which were less than the range of the VCIE. During the Cretaceous the carbon isotopic fractionation of carbonates varied from 1‰ to 3‰ and for TOC it varied from -29‰ to -25‰; and the carbon isotope fractionation between carbonate and TOC varied from -31 to -27 (HAYES *et al.*, 1999: Fig. 3).

Prior to defining subunits of the VCIE in the thick Koyamada Formation, the excursion in the ODP692 section was divided into three subunits (CAVALHEIRO *et al.*, 2021: Fig. 2). In the ODP692 core the VCIE is a 7-8 m-thick, marine shale compared to the much thicker terrigenous Japanese section, in which divisions of the carbon isotope curve are expanded. Interval A in ODP692 is similar to the Onset interval in Japan, unit B is equivalent to subunits P1 and P2, and Interval C approximates unit P3 in Japan. The positions of VCIE subunits of the eight stratigraphic sections in this study vary but their ages are similar (Table 1).

Similarly, the Cenomanian-Turonian carbon isotope curve, OAE 2, is subdivided into subunits (LOWREY *et al.*, 2014; BEIL *et al.*, 2020), although the pattern differs from that of VCIE. The "ramp-up" interval is a gradual increase of about 1.5‰ of bulk carbonate isotope and 3-4‰ of organic carbon isotope. The first positive peak is the initial enrichment ("A"), followed by a negative shift ("B"), which is followed by a sustained plateau ("C") (PRATT & THRELKELD, 1984). The upper boundary is the beginning of the return to the initial value. This configuration is documented in the North American Western Interior, western Europe and elsewhere (LOWERY *et al.*, 2014).

The upper Pliensbachian carbon isotope excursion in eastern Oregon, western United States, is divided into four negative-positive segments about 1‰ in organic carbon (DE LENA *et al.*, 2019). The initial negative excursion began during a warm period, and the succeeding positive-negative peaks were during a cool period. Radioisotope dates show that this excursion preceded the Karoo-Ferrar LIP and was not driven by that volcanic event.

Table 1. Stratigraphic sections with data of Valanginian CIE and data of four subunits in each section.

A. Data of Valanginian Carbon Isotope Excursion Chemozone

Sections	δ13C Sample	Sample Spacing	Position Meters		Thickness	Ages Ma		
		meters	Base	Top		Base	Top	Duration
DSDP 534A, W. Atlantic	Carbonate	~3	-1220	-1137	83 m	135.04	132.55	2.49 Myr
La Charce, France	Carbonate	~2	125	188	63 m	134.77	132.61	2.16 Myr
Orpierre, France	Carbonate	~1	97	232	135 m	135.14	132.80	2.34 Myr
Capriolo, Italy	Carbonate	~1.2	-129	-70	59 m	134.55	132.51	2.04 Myr
Wadi Miadin, Oman	Carbonate	0.3-1.0	55	73	18 m	135.03	132.85	2.18 Myr
ODP 692B, Weddell Sea	Organics	0.2	-91.5	-82	9.5 m	135.56	132.56	3 Myr
DSDP 603B, W. Atlantic	Carbonate	1.3	-1533	-1453	80 m	135.50	132.86	2.64 Myr
Japan Outcrop	Organics	0.5-2.0	80	270	190 m	~135.40	132.50	2.9 Myr
Average		**0.4-1.5**			**79.69 m**	**135.08**	**132.66**	**2.47 Myr**

B. VCIE Subunit Data

Sections	Onset Thickness	P1 Thickness m-Ma		P2 Thickness m--Ma		P3 Thickness m-Ma	
DSDP 534A, W. Atlantic	0.84 m	-1192	134.20	-1180	133.80	-1153	133.03
La Charce, France	0.8 m	150	133.91	170	133.22	179	132.90
Orpierre, France	0.3 m	129	134.55	148	134.25	161	134.05
Capriolo, Italy	0.89 m	-100	134.46	-90	133.84	-86	133.58
Wadi Miadin, Oman	0.4 m	59	134.60	65	134	67	133.70
ODP 692B, Weddell Sea	0.6 m	89.6	134.92	no data		85.6	133.69
DSDP 603B, W. Atlantic	0.93 m	-1505	134.55	-1500	134.43	-1495	134.08
Japan Outcrop	0.1 m	100	135.30	195	133.6	230	133.30
Average	**0.61 m**		**134.56**		**133.87**		**133.54**

Correlation of the VCIE subunits

The distinct pattern of the VCIE is documented in eight marine and non-marine sections, four of which illustrate the variation of the isotope curve (Fig. 8). The details of each curve are a function of sample spacing, which varied in each section.

The distinctive Valanginian $\delta^{13}C$ excursion and its four subunits defined in the Koyamada Formation, Japan, are identified and correlated among four sections (Fig. 8). The $\delta^{13}C$ excursion increased abruptly and smoothly at most sites, remained a high plateau with several perturbations for about 2.7 Myr, then decreased slowly. The thicknesses and durations of the basal Onset interval vary greatly from section to section (Table 1). Its age differs by 1 Myr where it is oldest in the Weddell Sea DSDP 692 core and youngest in Capriolo, Italy. The Onset interval is thickest on the western Atlantic slope off North America and thinnest in Japan section. The diachroneity of the four subunits may in part be a function of sample spacing, inconsistency in identifying unit boundaries and of imprecision in interpolating numerical ages, and not necessarily a clue to the differential oceanic and atmospheric distribution and migration of $\delta^{13}C$. Beginning at the first high peak P1, the carbon isotope values remained steady at about 3‰ above the preceding background level. Multiple negative shifts of about 2‰ separate P1 through P3 subunits (Figs. 8-9). The interval between the base of P1 to the end of P3 lasted on average 1.02 Myr. Following the end of P3, the $\delta^{13}C$ values decreased gradually to about 1‰ above the prior background level.

A second cross section correlates an oceanic slope section in the western Atlantic with a shallow epicontinental basin in France and a carbonate slope in Oman with a lacustrine section in China (Fig. 9). The durations of the Onset and P1 intervals are variable, but subunits P2 and P3 are more consistent (Fig. 9; Table 1).

In the Luanping Basin, northeastern China, a positive ~3‰ $\delta^{13}C_{org}$ excursion is developed in the lacustrine facies (TONG *et al.*, 2024). The Dabeigou Formation is composed of non-marine fan-delta sandstone and lacustrine mudstone and sandstone. Fresh black mudstone was sampled at intervals of about 0.5 m spanning the carbon shift. The VCIE curve spans 70 m and consists of three strong positive peaks, here identified as P1 at 124 m, P2 at 140 m and P3 at 158 m directly overlying the youngest dated tuff bed (Fig. 9). The base of the Onset interval is at a negative shift at 108 m. Its age is constrained by four U-Pb zircon radioisotope ages in tuffs. Dates underlying the excursion in the underlying Zhangjiakou Formation are 134.5±0.4 Ma and 134.1±1.0 Ma. A tuff bed in the excursion in Member 3 lacustrine facies is dated at 131.5±0.4 Ma and 130.5±0.4 Ma. These radioisotope dates are about 1 Myr younger than ages of the chemozone in the Japanese section; this difference needs further research. Three TOC peaks of about 1% underlie and overlie the CIE. Within the CIE are minor TOC increases of about 0.25-0.3%. The low TOC and organic geochemistry support the conclusion that lake waters were mainly oxic to suboxic and related to declining photosynthetic fractionation and reduced atmospheric pCO_2 (TONG *et al.*, 2024).

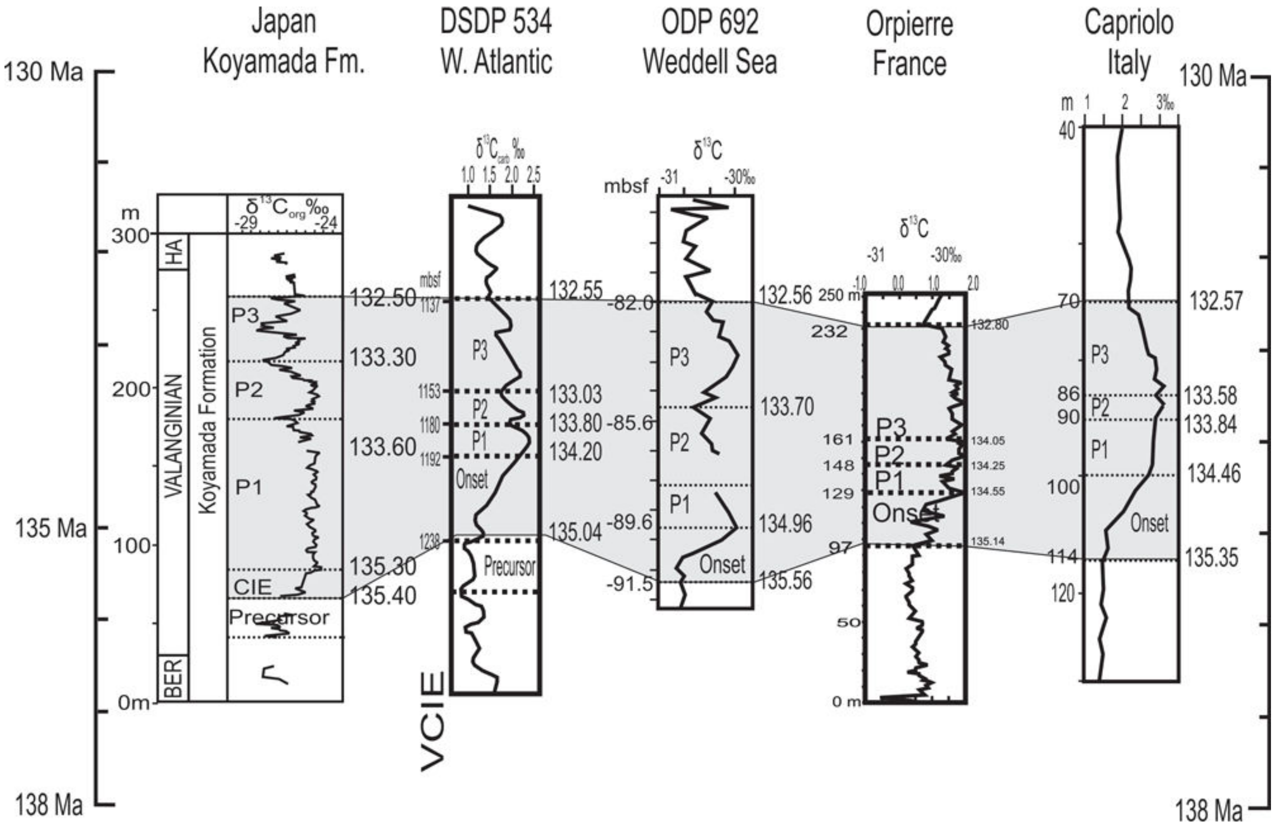

Figure 8: Chemozone correlation of four VCIE subunits (gray zone) defined in Japan with isotope curves in sections in north central Tethys, west central Atlantic and offshore Antarctic showing variations of the curve and boundary positions. Numerical ages of subunit boundaries were derived by ploting biostratigraphic data of the four sections to the CRET25 database.

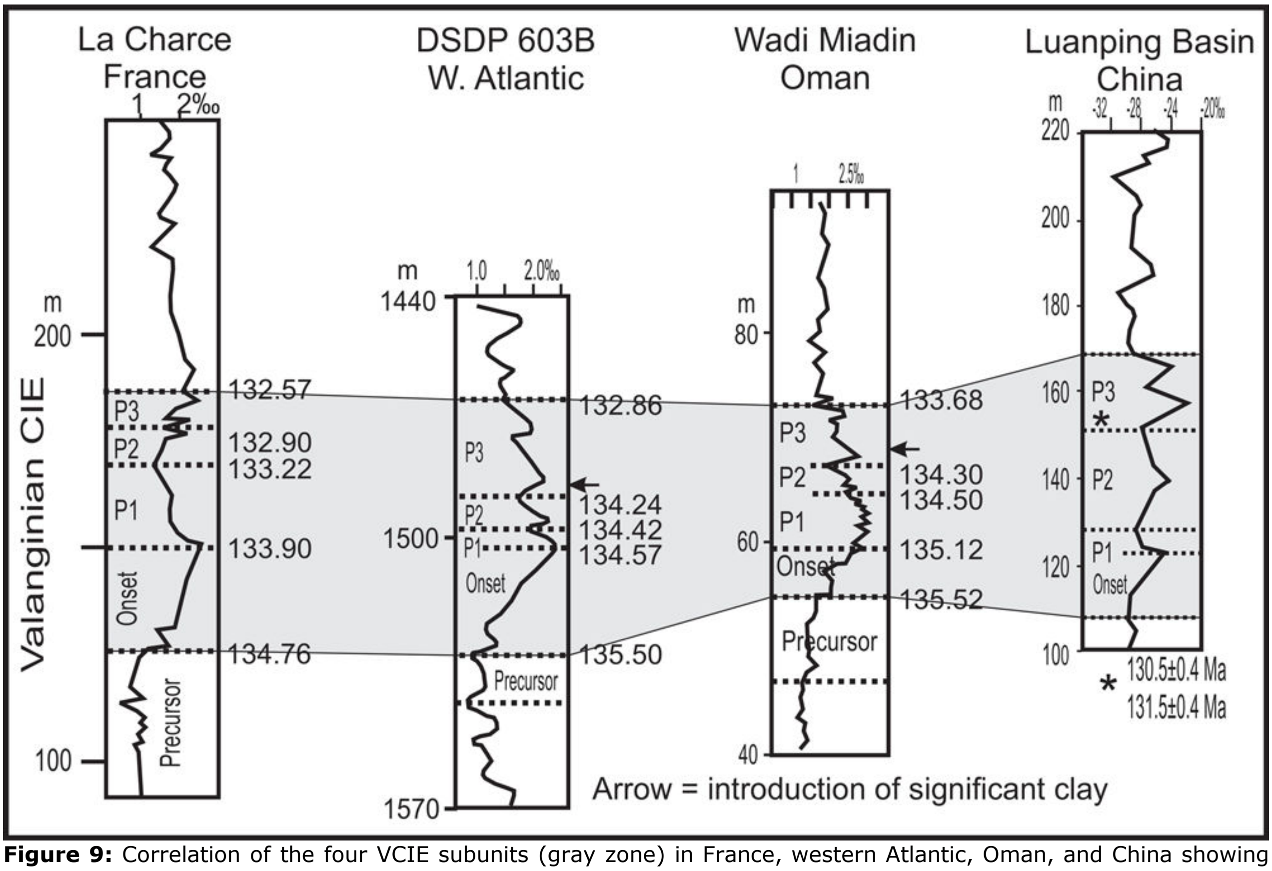

Figure 9: Correlation of the four VCIE subunits (gray zone) in France, western Atlantic, Oman, and China showing variations of the curve and boundary positions. Numerical ages were interpolated by projecting the subunit boundaries into the CRET25DB. In the Luanping Basin section, the asterix indicates position of tuff bed with two radioisotope dates (TONG *et al.*, 2024).

A well documented terrestrial example of the VCIE is in the Western Interior of North America at Utahraptor Ridge, Utah (Joeckle *et al.*, 2023). The Yellow Cat Member of the Lower Cretaceous Cedar Mountain Formation is a classic dinosaur locality replete with interbedded pedogenic layers. A 10 m-thick interval in the Yellow Cat Member was sampled at 0.27 m intervals and yielded a detailed $\delta^{13}C_{org}$‰ curve with three prominent peaks and ending at a 1.7‰ positive limb suggestive of another peak; this limb is overlain by a covered interval (Joeckle *et al.*, 2023: Fig. 5). The Yellow Cat Member is correlated with Berriasian to Hauterivian stages by palynologic, ostracod and charophyte data. The Early Cretaceous spore, *Foraminisporis wonthaggiensis*, was also reported in Spitsbergen (Jelby *et al.*, 2020). Volcanogenic zircons from a paleosol in the middle of the carbon curve were dated at 135.1±0.3 Ma (Joeckle *et al.*, 2023). This part of the Yellow Cat curve would correlate with subunit P2 in Japan, which is dated at 133.6 Ma.

In the Lower Saxony Basin, northern Germany, the Valanginian CIE is recorded in a Lower Cretaceous regressive-transgressive cored sequence (Thöle *et al.*, 2020). Coincident with the beginning of the carbon isotope excursion sea-level regression is indicated by high Si/Al ratios and sandstone strata. Thus, the VCIE began during high terrigenous sediment supply in this basin and continued as terrigenous sediment supply declined. The positive $\delta^{13}C_{org}$ excursion is correlated with the Valanginian by Boreal nannofossil zones and began in the transition from uppermost lower to upper Valanginian. The positive carbon excursion is about 3‰ and has multiple small shifts of about 1‰. Weight-percent organic matter ranges no more than 1% suggesting aerobic to dysaerobic conditions. The configuration of the curve defines five smaller offsets that compare well with the three major peaks in Japan.

In Spitsbergen the "Weissert Event" is identified in dark gray shale and siltstone of the Rurikfjellet Formation at a 3.5‰ positive shift in $\delta^{13}C_{org}$ (Jelby *et al.*, 2020). The excursion begins at a maximum flooding, condensed interval overlying the Volgian/Berriasian Agardhfjellet Formation, which is dated by Ryazanian ammonites. Lower Valanginian dinoflagellates date the lower 50 m of the excursion (Śliwińska *et al.*, 2020), and its upper part is dated by the upper Valanginian-Hauterivian belemnite, *Arctoteuthis bluethgeni* Doyle (Alsen *et al.*, 2020), which is overlain by Hauterivian dinoflagellates. The dinoflagellate assemblage is widespread in the Volga Basin and Western Europe and integrated with ammonites (Harding *et al.*, 2011). The carbon isotope curve, however, differs from other VCIE curves in that above the 3‰ positive shift, the curve remains a plateau through the Hauterivian with few small broad wobbles less than 1‰ but no significant positive or negative peaks.

5. Chronostratigraphy

Correlation with Lower Cretaceous ammonite zones

The La Charce outcrop, Vocontian Basin, France, integrates ammonites with the VCIE (Fig. 9). The lower-upper Valanginian boundary in this outcrop is placed between the single occurrence of the lower Valanginian *Neocomites platycostatus* Subzone at 1 m and the first occurrence of the upper Valanginian *Neocomites peregrinus* Zone at 24 m, which is directly below the base of the VCIE. In the CRET25DB the FAD of *N. peregrinus* is projected at 134.96 Ma. Previously, the base of the carbon excursion was correlated with the lower Valanginian *Karakaschiceras inostranzewi* Zone to the *Saynoceras verrucosum* Zone (Hennig *et al.*, 1999: Martinez *et al.*, 2023).

The VCIE was correlated with lower to upper Valanginian in the Pont de Carajuan, France, section (Fig. 10) (Hennig *et al.*, 1999; Weissert *et al.*, 2008), although the biostratigraphic data are inconclusive. This basin-margin section is divided into seven Valanginian and five Hauterivian sequences. The upper stage boundary is a significant disconformity that truncates uppermost Valanginian ammonite zones and the upper part of the VCIE; and basal Hauterivian zones are condensed (Arnaud & Bulot, 1992). The lower-upper Valanginian boundary is indeterminate because ammonite samples are widely spaced and some species are long ranging (Fig. 11). The lower Valanginian *Busnardoites campylotoxus* Zone is overlain by the upper Valanginian *Saynoceras verrucosum* Zone by a 35 m-thick interval (Arnaud & Bulot, 1992); intervening samples yielded two long-ranging species, *Olcostephanus guebhardi* and *Neocomites teschenensis* (Company & Tavera, 2015). Furthermore, the lower forty meters of the carbon isotope curve in the Pont de Carajuan section is a long rising line with no excursions except for a 0.3‰ negative blip in the lowermost 3 m (Fig. 11). The first positive excursion of 1.5‰ at 40 m equates with 84 m in the upper Valanginian part of the measured section and here is identified as P1; the base of the Onset phase is indistinguishable. The uppermost curve interval from 55 to 65 m at the unconformity is a single peak, which may be the lower of two P3 peaks in the Japan section (Fig. 11). The upper part of the carbon isotope curve apparently is cut out by the unconformity, which is directly overlain by the lower Hauterivian *Acanthodiscus radiatus* Zone. Thus, the carbon isotope curve in the Pont de Carajuan section correlates with only part of the Koyamada curve and the positive excursions are above the base of the *Saynoceras sayni* Zone marker in the lower Hauterivian.

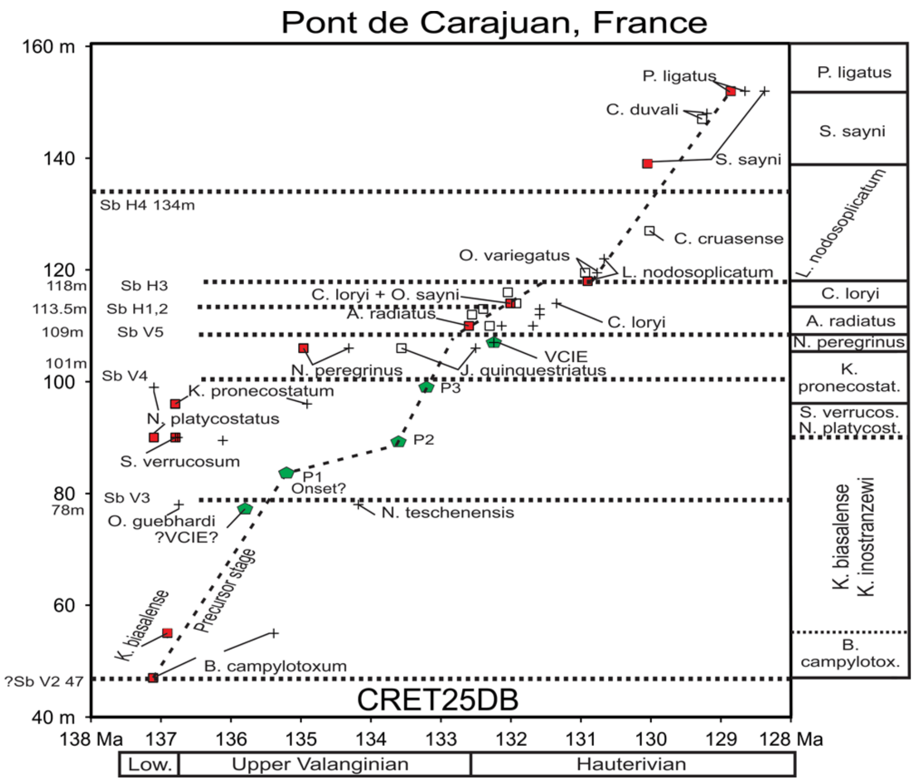

◀ **Figure 10:** Graphic plot of the Pont de Carajuan section to the CRET25DB. Sequence boundaries and fossil samples are from ARNAUD and BULOT (1992). Red rectangle makes position of key Valanginian taxon; green symbols mark base and top of carbon isotope excursion.

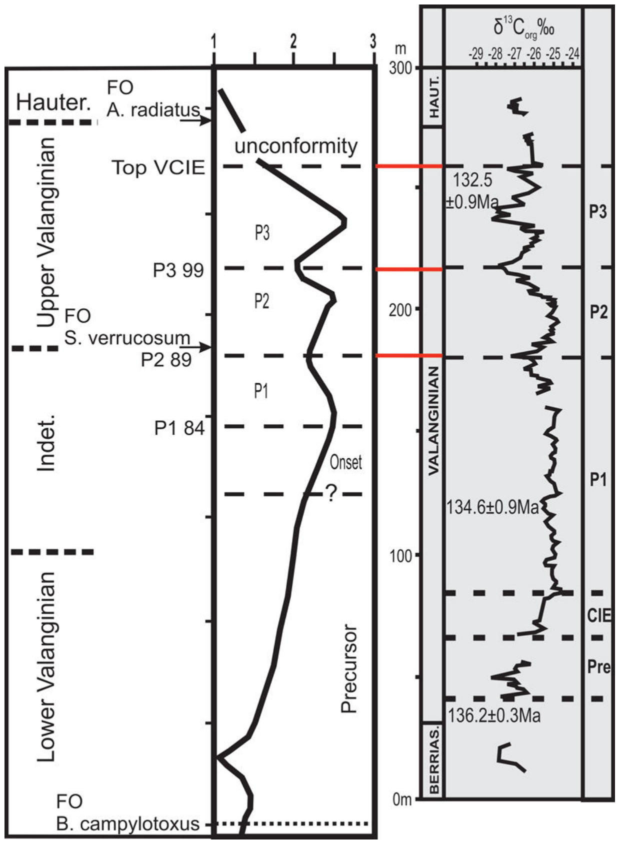

Figure 11: Correlation of the carbon curve at the Pont de Carajuan section (HENNIG *et al.*, 1999) with the curve in the Koyamada Formation, Japan (gray zone) (TOMARU *et al.*, 2025). The measured lithologic section is 152 m thick (ARNAUD & BULOT, 1992) and the carbon curve is 74 m thick, in which 0 m equals 47 m in the lithologic section.

Eight of the 124 stratigraphic sections in the CRET25DB are plotted to the CRET25DB in order to project the age of the boundaries of the Valanginian carbon isotope excursion (Table 1). The projected ages vary slightly because in several X/Y plots, more than one correlation line of interpretation is possible as constrained by the FADs/LADs of ammonites, calcareous nannofossils, calpionellids, and dinoflagellates. The age of VCIE ranges from 135.79 Ma to 132.25 Ma averaging 2.47 Myr in duration and lasting up to 2.90 Myr in Japan (Fig. 7; Table 1). The average age of the base is 135.08 Ma and the top is 132.66 Ma. The thicknesses of the excursion range from 190 m to 9.5 m and average 79.69 m. The average age of base P1 is 134.56 Ma, of P2 is 133.88 Ma and of P3 is 133.54 Ma. The lacustrine section in the Luanping Basin, China, was not included in this list of sections, because the date of the "P3" subunit is 2 to 3 Myr younger at 131.5±0.4 to 130.5±0.4 Ma, which correlates it with the Hauterivian Stage.

Integration with Cretaceous Time Scale

The Valanginian Stage spans from the FO of *Calpionellites darderi* (FAD 137.71 Ma) to the base of *Acanthodiscus radiatus* (FAD 132.60 Ma) at base of the Hauterivian Stage (GALE *et al.*, 2020; SZIVES *et al.*, 2024) (Fig. 12). In the Tethys Realm the base of the Valanginian is also defined by the "*Thurmanniceras*" *pertransiens* Zone, FAD 137.71 Ma, and the *Neocomites premolicus* Subzone (SZIVES *et al.*, 2024). The CRET25DB projects the FADs of both species at 137.71 Ma. The duration of the Valanginian as calculated by

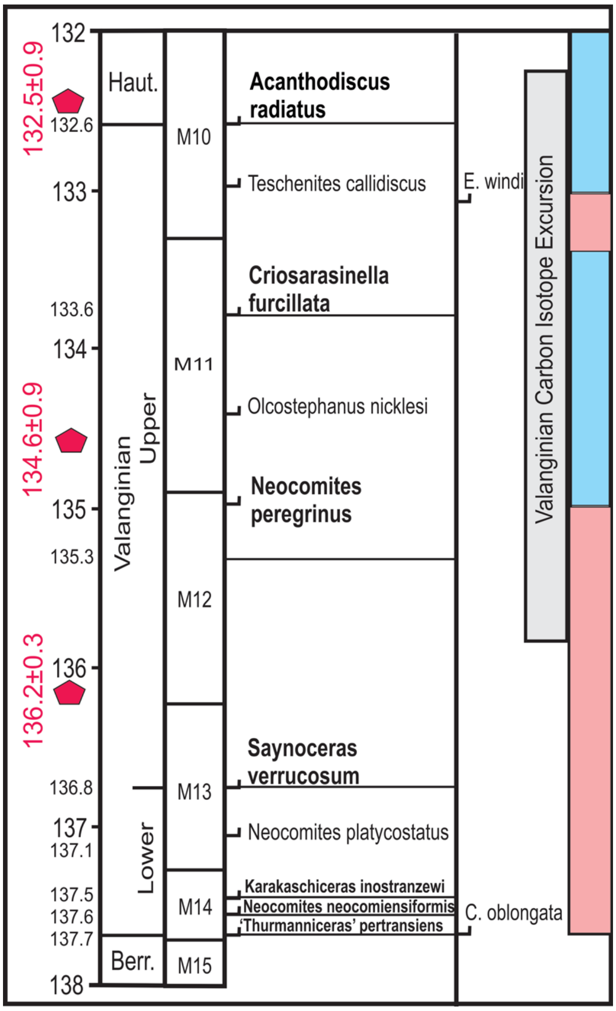

Figure 12: Correlation of Upper Valanginian Carbon Isotope Excursion with ammonite and calcareous nannofossil FADs and polarity chrons in CRET25 Chronostratigraphic Database. Bold names are standard ammonite zones (SZIVES *et al.*, 2024). Red symbols in left-hand column are dates from Japan; right-hand color bar marks warm (rose) and cool (blue) climates.

astrochronological methods ranges from 4.7 to 7.7 Myr (CHARBONNIER *et al.*, 2013; MARTINEZ *et al.*, 2023). In the CRET25DB the duration of the Valanginian Stage is 5.11 Myr from the FAD of *C. darderi* at 137.71 Ma to the FAD of *A. radiatus* at 132.60 Ma.

The VCIE chemozone spans from the upper Valanginian *Saynoceras verrucosum* Zone to the basal Hauterivian *Acanthodiscus radiatus* Zone (Fig. 12). The VCIE spans the FADs of two nannofossil bioevents, *Calcicalathina oblongata* at the base and *Eiffellithus windi* near the top. It spans Polarity Chrons M12 to M10. In the Japanese section the age of VCIE is dated from 135.40 Ma to 132.50 Ma, and thus, overlaps the beginning of the Hauterivian Stage at 132.60 Ma. At the La Charce section the base of the VCIE is in the lower part of the upper Valanginian in the *Neocomites peregrinus* Zone and 1 m above the FO of the zone species. Two astrochronological studies dated the Valanginian CIE beginning at 135.22±1.0 Ma with a duration of 5.85 Myr (MARTINEZ *et al.*, 2015); a later study revised it to 134.56±0.19 Ma (MARTINEZ *et al.*, 2023). TOMARU *et al.* (2025) dated the beginning between 136.2±0.3 and 134.6±0.9 Ma by radioisotope dates in volcanic material.

6. Early Cretaceous atmospheric and oceanic climate and tectonism

During latest Jurassic into earliest Cretaceous, from the Oxfordian Age into the early Valanginian, about twenty-five Myr, the $\delta^{13}C_{carb}$ of bulk sediment became progressively lighter by about 2‰ (Fig. 10) (PRICE *et al.*, 2016). Among several processes, burial of more negative carbon produced by photosynthesis in an oligotrophic, epipelagic/photic zone was likely (FALKOWSKI *et al.*, 2004). During this same time interval, the $^{87}Sr/^{86}Sr$ ratio increased uniformly from about 0.706900 to about 0.707500 (PRICE *et al.*, 2016), which suggests progressively increasing weathering. During Late Jurassic and Early Cretaceous calcite precipitation was favored over aragonite because the Mg/Ca ratio fell below 2 (MÜLLER *et al.*, 2013). This was during the beginning of continental separation and opening of the northern Atlantic Ocean (SCOTESE *et al.*, 2024).

Temperature

Oceanic temperature histories during the Valanginian $\delta^{13}C$ excursion have been carefully evaluated by multiple methods. Sea-surface temperatures (SST) were measured by foraminiferal successions, oxygen isotopes and Tex_{86} measurements on marine archaeal membrane lipids in organic matter (GRÖCKE *et al.*, 2005; MÖLLER *et al.*, 2015, 2020; O'BRIEN *et al.*, 2017; CAVALHEIRO *et al.*, 2021; HE *et al.*, 2025).

Since Late Jurassic, global climate slowly warmed into Early Cretaceous from slightly less than 20°C to slightly above 30°C (GODDÉRIS *et al.*, 2020; SCOTT & LINDSEY, 2025). Early Cretaceous atmospheric temperatures fluctuated, decreasing slightly during early Berriasian, then cooled dramatically in later Berriasian and into late Valanginian and early Hauterivian (Fig. 3). Tethys belemnite data show a stepwise temperature decrease throughout the Valanginian and into early Hauterivian, which is followed by warming (PRICE *et al.*, 2016). Integrated global paleotemperature data show that globally mean SST dropped 3.0±1.7°C from late Valanginian into early Hauterivian (CAVALHEIRO *et al.*, 2021; HE *et al.*, 2025). Also, atmospheric pCO_2 decreased during this time-period. At high latitudes (>±48° latitude) Valanginian SST ranged from about 22°C to 23 °C at least 10°C cooler than at low latitudes and possibly as great as 20°C (GRÖCKE *et al.*, 2005; MÖLLER *et al.*, 2015, 2020; O'BRIEN *et al.*, 2017; HE *et al.*, 2025). Low-latitude ocean temperature slightly increased from less than 25°C to 30°C; then decreased into the Hauterivian followed by a slight increase into early Aptian and then decreased again into latest Aptian. However, in offshore Antarctica at paleolatitude ~54° S and at a paleowater depth of ~500 meters, the temperature dropped 3-4°C during the late Valanginian CIE (Cavalheiro *et al.*, 2021). Multiple Valanginian-early Hauterivian continental glaciation events are documented in Australia while it was docked with Antarctica (Alley *et al.*, 2020).

The oceanic temperature off the coast of Antarctica at a paleolatitude of 54° S cooled during the four Valanginian carbon isotope subunits of the VCIE (Alley *et al.*, 2020; Cavalheiro *et al.*, 2021; He *et al.*, 2025). The carbon isotope curve in the ODP 692B core, Weddell Sea, spans 14 m of thin-laminated black shale (Fig. 8) (Cavalheiro *et al.*, 2021). This pattern is documented across all latitudes (Cavalheiro *et al.*, 2021).

The TEX_{86} curve records the warmest interval at the beginning of VCIE from the Onset into the P1 interval (Cavalheiro *et al.*, 2021). Then SST dropped nearly 5°C into the early part of P3 stage. By the end of the VCIE temperature warmed 3-4°C briefly. This warm-cool-warm-cool alternation is also documented in Madagascar by belemnites, oysters and bulk carbonate (He *et al.*, 2025). Unlike younger Cretaceous carbon isotope excursions when ocean anoxia developed, oceanic conditions during the VCIE fluctuated between oxic and dysaerobic conditions (Percival *et al.*, 2023; Tomaru *et al.*, 2025).

Humidity and productivity

During the earliest Valanginian and into the Valanginian-Hauterivian transition, climate was humid and marine productivity increased as documented by clay minerals, palynological and calcareous nannofossil assemblages (Duchamp-Alphonse *et al.*, 2007; Kujau *et al.*, 2012, 2013; Morales *et al.*, 2013; Bodin *et al.*, 2015; Price *et al.*, 2016; Charbonnier *et al.*, 2020; Percival *et al.*, 2023).

Surface-water productivity as indicated by calcareous nannofossils and elevated Sr/Ca ratios in the west-central Atlantic recorded in DSDP 534A, was high during Berriasian-mid-Valanginian into the Onset phase about 135 Myr, then decreased into latest Valanginian (Casellato *et al.*, 2008: Fig 2; Percival *et al.*, 2023). In the southern ocean Weddell Sea, ODP 692B, ocean temperature was warmest prior to and during the Onset of VCIE and cooled beginning about P1 into the recovery phase after P3 to the end of the Valanginian (Cavalheiro *et al.*, 2021). On the southeast margin of the Arabian platform prograding into the Rayda Basin, Jebal Akhdar, Oman (Dujoncquoy *et al.*, 2018), terrigenous influx increased at about 134.00 Ma when deposition of the argillaceous Salil Formation began (Scott, 1990; Celestino *et al.*, 2016). The $\delta^{18}O$ also decreased from -3‰ to less than -4‰ suggesting a small temperature decrease, which was inferred by Dujoncquoy *et al.* (2018). About the same time on the western margin of the Central Atlantic, increased terrigenous influx during P3 subunit is also dated at 134.00 Ma (Figs. 8-9, arrows). This is consistent with a return to global humid climate as ocean temperatures cooled. Following the end of VCIE, as recorded in DSDP 534A, terrigenous influx increased suggesting sea-level changes (Cotillon, 1992) or more humid climate (Lini *et al.*, 2007; Percival *et al.*, 2023) or both. In East Texas the upper Valanginian-lower Hauterivian terrigenous Hosston Formation overlies the drowned lower Valanginian carbonate ramp, Knowles Limestone (Mann & Thomas, 1964; Mancini *et al.*, 2012; Scott, 2019), which supports the regional extent of latest Valanginian increased terrigenous sedimentation and the rise of climate humidity. Late Valanginian Osmium isotope ($^{187}Os/^{188}Os$) preceding VCIE and into the Onset stage suggests that weathering of Paraná-Etendeka basalt increased influx of micronutrients, which fertilized the oceans (Percival *et al.*, 2023). Manganese and iron are enriched in Valanginian carbonates in the Mediterranean and Atlantic suggesting elevated continental weathering and expansion of dysoxic water masses (Kuhn *et al.*, 2005).

It appears that during the Tithonian Stage, calcite precipitation was favored because pCO_2 was reduced and SST temperature warmed and photosynthesis was active (Dreybrodt *et al.*, 1997). Aragonite tends to be precipitated faster than calcite at a given state (Mucci *et al.*, 1989). These conditions changed during VICE resulting in dissolution of some pelagic organisms.

Southern volcanic Large Igneous Province (LIP)

The Paraná-Etendeka LIP was apparently the main trigger of the Valanginian carbon isotope excursion (Martinez *et al.*, 2015, 2023; Celestino *et al.*, 2016; Gomes & Vasconcelos, 2021; Percival *et al.*, 2023; Tomaru *et al.*, 2025). Recent studies based on high-precision radioisotopes date the emplacement spanning from 135.0±0.6 to 133.2±0.3 Ma (Gomes & Vasconcelos, 2021). The timing coincidence of Paraná Continental Flood Basalt formation suggests that it impacted the Valanginian CIE (Jelby *et al.*, 2020; Thöle *et al.*, 2020; Joeckle *et al.*, 2023; Tong *et al.*, 2024). In the Japanese section the VCIE is bracketed by precise radioisotope dates on volcanic ash at 136.2±0.3 Ma and 132.5±0.9 Ma, which are consistent with new dates of these flood basalts.

7. Conclusions

The Late Jurassic-Early Cretaceous Phytoplankton Ecosystem Evolution and its associated Calcification Event were major evolutionary innovations that fundamentally altered the global oceanic marine pelagic zone. Pelagic micro-organisms, nannoflora, dinoflagellates and calpionellids, constructed tests out of calcium carbonate and diversified becoming abundant producers in the Late Jurassic-earliest Cretaceous seas. Phytoplankton diversification was detoured by the Valanginian CIE chemozone, when nannoconid diversity and abundance decreased along with dinoflagellates and calpionellids. Ocean chemistry and temperature fluctuated following volcanic eruptions of the Paraná-Etendeka LIP.

The VCIE is a global chronostratigraphic chemozone composed of four subunits that are documented in the Koyamada Formation, Japan, in the west Pacific Ocean. These four subunits of the VCIE are identified in eight globally widespread sections. The VCIE began during the late Valanginian *Neocomites peregrinus* Zone and ended in the *Acanthodiscus radiatus* Zone in the earliest Hauterivian; the recovery stage continued into the earliest part of the Hauterivian Stage. The VCIE chemozone spanned from M11r Polarity Chron into M10N Polarity Chron.

The Valanginian carbon isotope chemozone began with the Onset subunit at 135.79 Ma and ended at the end of subunit P3 at 132.25 Ma. This chemozone coincided with the emplacement of the Paraná-Etendeka LIP dated from 135.0±0.6 to 133.2±0.3 Ma. The duration of the Paraná-Etendeka LIP was a minimum of 1.8 Myr, and the average duration of the VCIE was 2.47 Myr. ERBA and TREMOLADA (2004) estimated the duration of VCIE at about 2 Myr. This Valanginian carbon excursion is related to significant changes in the atmosphere and hydrosphere and to a major change in marine biota and ecosystems. The decrease of calcareous nannoconids and virtual extinction of calpionellids formed the first Cretaceous marine biotic crisis that influenced subsequent Cretaceous marine biota.

Acknowledgements

We acknowledge the fundamental stratigraphic research by many teams who acquired and interpreted the voluminous data. Understanding the biotic changes that preceded the Valanginian isotope excursion have matured since Helmut WEISSERT and colleagues discovered it in the 1980's. Apology to Dr. WEISSERT for editing the name of this carbon isotope event so its name is consistent with names of younger Cretaceous events. Erik POLLOCK, the University of Arkansas Stable Isotope Laboratory, helped in the processing and interpretation of the carbon isotope data. Colleagues Carl BRETT, Rick FLUEGEMAN, Ed LANDING, and Brian PRATT helped to clarify and promote the concept of chemozone as an important stratigraphic unit. Anonymous reviewers recommended important changes and current research that upgraded the study of the Late Jurassic and Early Cretaceous biotic changes and of the Valanginian carbon isotope chemozone.

Declaration of competing interests

This research did not receive specific grants from funding agencies in the public, commercial, or not-for-profit sectors. AI tools were employed in searching the literature but not the gathering of data, nor in its manipulation or in preparing illustrations or writing. In research using Google Tools, Google AI summaries were examined before searching for resource publications.

Bibliographic references

AGUADO R., GEA G.A. de & O'DOGHERTY L. (2014).- Integrated biostratigraphy (calcareous nannofossils, planktonic foraminifera, and radiolarians) of an uppermost Barremian-lower Aptian pelagic succession in the Subbetic Basin (southern Spain).- *Cretaceous Research*, vol. 51, p. 153-173.

ALLEY N.F., HORE S.B. & FRAKES L.A. (2020).- Glaciations at high-latitude Southern Australia during the Early Cretaceous.- *Australian Journal of Earth Sciences*, vol. 67, no. 8, p. 1045-1095. DOI: 10.1080/08120099.2019.1590457

ALSEN P., JELBY M.E., ŚLIWIŃSKA K.K. & MUTTERLOSE J. (2020).- An Early Cretaceous stratigraphic marker fossil in the High Arctic: The belemnite *Arctoteuthis bluethgeni*.- *Geological Magazine*, vol. 157, Special Issue 10, p. 1715-1728

ANDREINI G., CARACUEL J. & PARISI G. (2007).- Calpionellid biostratigraphy of the Upper Tithonian-Upper Valanginian interval in Western Sicily (Italy).- *Swiss Journal of Geosciences*, vol. 100, p. 179-198. DOI: 10.1007/s00015-007-1227-z

ARNAUD H. & BULOT L.G. (1992).- Provence platform (Berriasian to Barremian) : Early Cretaceous backstepping, faunal renewals and séquence stratigraphy. *In*: ARNAUD H. & LEMOINE M. (eds.), Alpine Mesozoic basin in the South-East of France.- *Field-Course of the American Association of Petroleum Geologists*, Nice, vol. C5, p. 109-133.

ATASOY G., ALTINER D. & ÖZKAN-ALTINER S. (2022).- Calibrating the Late Jurassic-Early Cretaceous shallow and deep marine bioevents by quantitative biostratigraphy: A synthesis from the Pontides Carbonate Platform (Turkey).- *Earth-Science Reviews*, vol. 231, article 104071, 41 p.

BEIL U.S., KUHNT W., HOLBOURN A., SCHOLZ F., OXMANN J., WALLMANN K., LORENZEN J., AQUIT M. & CHELLAI E.H. (2020).- Cretaceous oceanic anoxic events prolonged by phosphorus cycle feedbacks.- *Climate of the Past*, vol. 16, no. 2, p. 757-782. DOI: 10.5194/cp-16-757-2020

BENZAGGAGH M. (2021).- Systematic revision and evolution of the Tithonian family Chitinoidellidae TREJO, 1975.- *Carnets Geol.*, vol. 21, no. 2, p. 27-53. DOI: 10.2110/carnets.2021.2102

BERGEN J.A. (1994).- Berriasian to Early Aptian calcareous nannofossils from the Vocontian Trough (SE France) and Deep Sea Drilling Site 534: New nannofossil taxa and a summary of low-latitude biostratigraphic events.- *Journal of Nannoplankton Research*, vol. 16, no. 2, p. 59-69.

BODIN S., CHARPENTIER M., ULLMANN C.V., RUDRA A. & SANEI H. (2023).- Carbon cycle during the late Aptian-early Albian OAE 1b: A focus on the KILIAN-PAQUIER levels intervals.- *Global and Planetary Change*, vol. 222, article 104074, 17 p. DOI: 10.1016/j.gloplacha.2023.104074

BODIN S., MEISSNER P., JANSSEN N.M.M., STEUBER T. & MUTTERLOSE J. (2015).- Large igneous provinces and organic carbon burial: Controls on global temperature and continental weathering during the Early Cretaceous.- *Global and Planetary Change,* vol. 133, p. 238-253

BORNEMANN A. & MUTTERLOSE J. (2008).- Calcareous nannofossil and $\delta^{13}C$ records from the Early Cretaceous of the western Atlantic Ocean: Evidence for enhanced fertilization across the Berriasian-Valanginian transition.- *Palaios*, vol. 23, no. 12, p. 821-832.

BOTTINI C., DIENI I., ERBA E., MASSARI F. & WEISSERT H. (2018).- The Valanginian WEISSERT Oceanic Anoxic event recorded in Central-Eastern Sardinia (Italy).- *Rivista Italiana di Paleontologia e Stratigrafia (Research in Paleontology and Stratigraphy)*, vol. 124, no. 3, p. 617-637. DOI: 10.13130/2039-4942/10740

BOWN P.R., LEES J.A. & YOUNG J.R. (2004).- Calcareous nannoplankton evolution and diversity through time. *In*: THIERSTEIN H.R. & YOUNG J.R. (eds.), Coccolithophores.- Springer, Berlin, Heidelberg, p. 481-508. DOI: 10.1007/978-3-662-06278-4_18

BOWN P.R., RUTLEDGE D.C., CRUX L.A. & GALLAGHER L.T. (1998).- Lower Cretaceous. *In*: BOWN P.R. (ed.), Calcareous nannofossil biostratigraphy.- Kluwer Academic Publishers, New York, p. 86-131.

CARNEY J.L. & PIERCE R.W. (1995).- Graphic correlation and composite standard databases as tools for the exploration biostratigrapher. *In*: MANN K.O. & LANE H.R. (eds.), Graphic correlation.- *SEPM Special Publication*, vol. 53, p. 23-43.

CASELLATO C.E., ANDREINI G., ERBA E. & PARISI G. (2008).- Calcareous Nannofossil and Calpionellid calcification events across the Tithonian-Berriasian time interval and low latitudes paleoceanographic implications. *In*: LEES J. (ed.), INA12, Lyon, France - Abstracts Volume.- *Journal of Nannoplankton Research*, Special Number, p. 33 (abstract). URL: https://ina.tmsoc.org/JNR/online/30/INA12%20ABSTRACTS%20JNR30S.pdf

CASELLATO C.E. & ERBA E. (2021).- Reliability of calcareous nannofossil events in the Tithonian-early Berriasian time interval: Implications for a revised high resolution zonation.- *Cretaceous Research*, vol. 117, article 104611, 30 p.

CAVALHEIRO L., WAGNER T., STEINIG S., BOTTINI C., DUMMANN W., ESEGBUE O., GAMBACORTA G., FARNSWORTH A., FLÖGEL S., HOFMANN P., LUNT D.J., RETHEMEYER J., TORRICELLI S. & ERBA E. (2021).- Impact of global cooling on Early Cretaceous high pCO_2 world during the WEISSERT Event.- *Nature Communications*, vol. 12, article 5411, 11 p. DOI: 10.1038/s41467-021-25706-0

CELESTINO R., WOHLWEND S., REHÁKOVA D. & WEISERT H. (2016).- Biostratigraphy and sedimentology of the Upper Jurassic-Lower Cretaceous Rayda Formation, central Oman Mountains.- *Newsletters on Stratigraphy*, vol. 50, no. 1, p. 91-109.

CHANNEL J.E.T., CECCA F. & ERBA E. (1995).- Correlation of Hauterivian and Barremian (Early Cretaceous) stage boundaries to polarity chrons.- *Earth and Planetary Science Letters*, vol. 134, nos. 1-2, p. 125-140.

CHARBONNIER G., BOULILA S., GARDIN S., DUCHAMP-ALPHONSE S., ADATTE T., SPANGENBERG J.E., FÖLLMI K., COLIN C. & GALBRUN B. (2013).- Astronomical calibration of the Valanginian "WEISSERT" episode: The Orpierre marl-limestone succession (Vocontian Basin, southeastern France).- *Cretaceous Research,* vol. 45, p. 25-42.

CHARBONNIER G., DUCHAMP-ALPHONSE S., DECONINCK J.F., ADATTE T., SPANGENBERG J.E., COLIN C. & FÖLLMI K.B. (2020).- A global palaeoclimatic reconstruction for the Valanginian based on clay mineralogical and geochemical data.- *Earth-Science Reviews*, vol. 202, article 103092, 17 p.

COMPANY M. & TAVERA J.M. (2015).- Lower Valanginian ammonite biostratigraphy in the Subbetic Domain (Betic Cordillera, southeastern Spain).- *Carnets Geol.*, Madrid, vol. 15, no. 8, p. 71-88. DOI: 10.4267/2042/56745

COTILLON P. (1992).- Search for eustacy record in deep Tethyan deposits through the study of sedimentary flux variations. Application to the Upper Tithonian-Lower Aptian series at DSDP Site 534 (central Atlantic).- *Palæogeography, Palæoclimatology, Palæoecoloogy*, vol. 91, nos. 3-4, p. 263-275.

COVINGTON M. & WISE S.W. Jr (1987).- 16. Calcareous nannofossil biostratigraphy of a Lower Cretaceous deep-sea fan complex: Deep Sea Drilling Project Leg 93 Site 603, Lower Continental Rise off Cape Hatteras.- *Initial Reports DSDP*, vol. XCIII, p. 617-660. DOI: 10.2973/dsdp.proc.93.116.1987

DE LENA L.F., TAYLOR D., GUEX J., BARTOLINI A., ADATTE T., ACKEN D. van, SPANGENBERG J.E., SAMANKASSOU E., VENNEMANN T. & SCHALTEGGER U. (2019).- The driving mechanisms of the carbon cycle perturbations in the late Pliensbachian (Early Jurassic).- *Scientific Reports, Nature Research*, vol. 9, article 18430, 12 p. DOI: 10.1038/s41598-019-54593-1

DREYBRODT W., EISENLOHR L., MADRY B. & RINGER S. (1997).- Precipitation kinetics of calcite in the system $CaCO_3$ H_2O $C0_2$: The conversion to CO_2 by the slow process $H^+ + HCO_3^- \rightarrow CO_2 + H_2O$ as a rate limiting step.- *Geochimica et Cosmochimica Acta,* vol. 61, no. 18, p. 3897-3904.

DUCHAMP-ALPHONSE S., GARDIN S., FIET N., BARTOLINI A., BLAMART D. & PAGEL M. (2007).- Fertilization of the northwestern Tethys (Vocontian basin, SE France) during the Valanginian carbon isotope perturbation: evidence from calcareous nannofossils and trace element data.- *Palæogeography, Palæoclimatology, Palæoecology,* vol. 243, nos. 1-2, p. 132-151. DOI: 10.1016/j.palaeo.2006.07.010

DUJONCQUOY E., GRÉLAUD C., RAZIN P., IMBERT P., BUCHEM F. van, DUPONT G. & LE BEC A. (2018).- Seismic stratigraphy of a Lower Cretaceous prograding carbonate platform (Oman) and implications for the eustatic sea-level curve.- *AAPG Bulletin*, vol. 102, no. 3, p. 509-543.

Erba E., Duncan R.A., Bottini C., Tiraboschi D., Weissert H., Jenkyns H.C. & Malinverno A. (2015).- Environmental consequences of Ontong Java Plateau and Kerguelen Plateau volcanism. *In*: Neal C.R., Sager W.W., Sano T. & Erba E. (eds.), The origin, evolution, and environmental impact of oceanic large igneous provinces.- *GSA Special Paper*, vol. 511, p. 271-303.

Erba E. & Tremolada F. (2004).- Nannofossil carbonate fluxes during the Early Cretaceous: Phytoplankton response to nutrification episodes, atmospheric CO_2, and anoxia.- *Paleoceanography,* vol. 19, no. 1, article PA1008, 18 p. DOI: 10.1029/2003PA000884

Falkowski P.G., Katz M.E., Knoll A.H., Quigg A., Raven J.A., Schofield O. & Taylor F.J.R. (2004).- The evolution of modern eukaryotic phytoplankton.- *Science,* vol. 305, no. 5682, p. 354-360.

Fraaije R.H.B., Van Bakel B.W.M. & Jagt J.W.M. (2018).- The rise of a novel, plankton-based marine ecosystem during the Mesozoic: A bottom-up model to explain new higher-tier invertebrate morphotypes.- *Boletín de la Sociedad Geológica Mexicana*, vol. 70, no. 1, p. 187-200. DOI: 10.18268/bsgm2018v70n1a11

Gale A.S., Mutterlose J. & Batenburg S. (2020).- Ch. 27. The Cretaceous Period. *In*: Gradstein F.M., Ogg J.G., Schmitz M.D. & Ogg G.M. (eds.), The Geologic Time Scale 2020, 2.- Elsevier, Amsterdam, p. 1023-1086.

Goddéris Y., Donnadieu Y. & Pohl A. (2020).- The Phanerozoic climate. *In*: Ramstein G., Landais A., Bouttes N., Sepulchre P. & Govin G. (eds.), Paleoclimatology.- Springer*,* Stuttgart, p. 359-383.

Gomes A.S. & Vasconcelos P.M. (2021).- Geochronology of the Paraná-Etendeka large igneous province.- *Earth-Science Reviews*, vol. 220, article 103716, 34 p.

Gradstein F., Gale A., Kopaevich L., Waskowska A., Grigelis A., Glinskikh L. & Görög Á. (2017).- The planktonic foraminifera of the Jurassic. Part II: Stratigraphy, palaeoecology and palaeobiogeography.- *Swiss Journal of Palaeontology*, vol. 136, no. 2, p. 259-271. DOI: 10.1007/s13358-017-0132-y

Granier B.R.C. (coordinator), Andreu Rodes J.M., Benzaggagh M., Blau J., Böker É., Estévez Rubio A., Ferré B., Lambert B.C., Marini A., Monteil E., Reboulet S. & Virgone A. (2024).- Rectifying a substantial biostratigraphic error: There are no Hauterivian calpionellids in Busot (Alicante, Spain).- *Carnets Geol.*, Madrid, vol. 25, no. 2, p. 29-72. DOI: 10.2110/carnets.2025.2502

Gréselle B., Pittet B., Mattioli E., Joachimski M., Barbarin N., Riquier L., Reboulet S. & Pucéat E. (2011).- The Valanginian isotope event: A complex suite of palaeoenvironmental perturbations.- *Palæogeograpy, Palæoclimatology, Palæoecology,* vol. 306, nos. 1-2, p. 41-57.

Gröcke R., Price G.D., Robinson S.A., Baraboshkin E.Y., Mutterlose J. & Ruffell A.H. (2005).- Upper Valanginian (Early Cretaceous) positive carbon-isotope event recorded in terrestrial plants.- *Earth and Planetary Science Letters*, vol. 240, no. 2, p. 495-509.

Habib D. & Drugg W.S. (1987).- 27. Dinoflagellate are of Middle Jurassic-Early Cretaceous sediments in the Blake-Bahama Basin.- *Initial Reports DSDP*, vol. LXXVI, p. 623-638. DOI: 10.2973/dsdp.proc.76.126.1983

Haq B.U. (2014).- Cretaceous eustasy revisited.- *Global and Planetary Change*, vol. 113, p. 44-58.

Harding I.C., Smith G.A., Riding J.B. & Wimbledon W.A.P. (2011).- Inter-regional correlation of Jurassic/Cretaceous boundary strata based on the Tithonian-Valanginian dinoflagellate cyst biostratigraphy of the Volga Basin, western Russia.- *Review of Palaeobotany and Palynology*, vol. 167, nos. 1-2, p. 82-116.

Hart M.B., Oxford M.J. & Hudson W. (2002).- The early evolution and palaeobiogeography of Mesozoic planktonic foraminifera. *In*: Crame J.A. & Owen A.W. (eds.), Palaeobiogeography and biodiversity change: The Ordovician and Mesozoic-Cenozoic radiations.- *GSL Special Publication*, vol. 194, p. 11-125.

Hayes J.M., Strauss H. & Kaufman A.J. (1999).- The abundance of ^{13}C in marine organic matter and isotopic fractionation in the global biogeochemical cycle of carbon during the past 800 Ma.- *Chemical Geology*, vol. 161, nos. 1-3, p. 103-125.

He S., Wang T., Spicer R.A., Farnsworth A., Mulch A., Widdowson M., Zhang Q., Cai F., Valdes P.J., Wang C., Randrianaly H.N., Xie J. & Ding L. (2025).- Back to an ice-free future: Early Cretaceous seasonal cycles of sea surface temperature and glacier ice.- *Science Advances*, vol. 11, article eadr9417, 13 p. DOI: 10.1126/sciadv.adr9417

Hennig S., Weissert H. & Bulot L. (1999).- The Valanginian C-isotope excursion: Calibration with ammonite stratigraphy.- *Geologica Carpathica*, vol. 50, no. 1, p. 91-96. URL: https://geologicacarpathica.com/browse/archive/?journal_article_no=2516

Hennig Fischer S. (2003).- Geochemical and sedimentological evidence for environmental changes in the Valanginian (Early Cretaceous) of the Tethys region.- Dissertation Nr. 15106, ETH Zurich,10.3929/ethz -a-004572748

Hull P.M. (2017).- Emergence of modern marine ecosystems.- *Current Biology*, vol. 27, no. 11, p. R466-R469. DOI: 10.1016/j.cub.2017.04.041

Ivanova D.K. & Kietzmann D.A. (2017).- Calcareous dinoflagellate cysts from the Tithonian - Valanginian Vaca Muerta Formation in the southern Mendoza area of the Neuquén Basin, Argentina.- *Journal of South American Earth Sciences*, vol. 77, p. 150-169.

Jelby M.E., Śliwińska K.K., Koevoet M.J., Alsen P., Vickers M.L., Olaussen S. & Stemmerik L. (2020).- Arctic reappraisal of global carbon-cycle dynamics across the Jurassic-Cretaceous boundary and Valanginian Weissert Event.- *Palæogeography, Palæoclimatology, Palæoecology*, vol. 555, article 109847, 18 p.

Joeckel R.M., Suarez C.A., McLean N.M., Möller A., Ludvigson G.A., Suarez M.B., Kirkland J.I., Andrew J., Kiessling S. & Hatzell G.A. (2023).- Berriasian-Valanginian Geochronology and Carbon-Isotope Stratigraphy of the Yellow Cat Member, Cedar Mountain Formation, Eastern Utah, USA.- *Geosciences,* vol. 13, no. 2, 18 p. DOI: 10.3390/geosciences13020032

Knoll A.H. & Follows M.J. (2016).- A bottom-up perspective on ecosystem change in Mesozoic oceans.- *Proceedings of the Royal Society B*, vol. 283, no. 1841, article 20161755, 10 p. DOI: 10.1098/rspb.2016.1755

Korte C., Hesselbo S.P., Ullmann C.V., Dietl G., Ruhl M., Schweigert G. & Thibault N. (2015).- Jurassic climate mode governed by ocean gateway.- *Nature Communications*, vol. 6, no. 10015, 7 p. DOI: 10.1038/ncomms10015

Kuhn O., Weissert H., Föllmi K. & Hennig S. (2005).- Altered carbon cycling and trace-metal enrichment during the late Valanginian and early Hauterivian.- *Eclogae geologicae Helvetiae*, vol. 98, no. 3, p. 333-344. DOI: 10.1007/s00015-005-1172-7

Kujau A., Heimhofer U., Hochuli P.A., Pauly S. & Mutterlose J. (2013).- Reconstructing Valanginian (Early Cretaceous) mid-latitude vegetation and climate dynamics based on spore-pollen assemblages.- *Review of Palaeobotany and Palynology,* vol. 197, p. 50-69.

Kujau A., Heimhofer U., Ostertag-Henning C., Gréselle B. & Mutterlose J. (2012).- No evidence for anoxia during the Valanginian carbon isotope event - An organic geochemical study from the Vocontian Basin, SE France.- *Global and Planetary Change*, vols. 92-93, p. 92-104.

Lini A., Weissert H. & Erba E. (2007).- The Valanginian carbon isotope event - a 1st episode of greenhouse climate conditions during the Cretaceous.- *Terra Nova*, vol. 4, no. 3, p. 374-384.

Lipps J.H., Stoedk T. & Dunthorn M. (2013).- Chapter 8. Fossil Tintinnids. *In*: Dolan J.R., Montagnes D.J.S., Agatha S., Coats D.W. & Stoecker D.K. (eds.), The biology and ecology of Tintinnid Ciliates: Models for marine plankton, first edition.- John Wiley & Sons Ltd., New York, p. 186-193.

Lowery C.M., Corbett M.J., Leckie R.M., Watkins D., Romero A.M. & Pramudito A. (2014).- Foraminiferal and nannofossil paleoecology and paleoceanography of the Cenomanian-Turonian Eagle Ford Shale of southern Texas.- *Palæogeography, Palæoclimatology, Palæoecology*, vol. 413, p. 49-65.

MacRae R.A., Fensome R.A. & Williams G.L. (1996).- Fossil dinoflagellate diversity, originations, and extinctions and their significance.- *Canadian Journal of Botany*, vol. 74, no. 11, p. 1687-1694.

Mancini E.A., Aharon P., Goddard D.A., Horn M. & Barnaby R. (2012).- Basin analysis and petroleum system characterization and modeling, interior salt basins, central and eastern Gulf of Mexico - Part 3: Tectonic/depositional history, resource assessment.- *AAPG Search and Discovery*, Article 10395, 111 p. URL: http://www.searchanddiscovery.com/documents/2012/10396mancini/mancini-part3.pdf

Mann J. & Thomas W.A. (1964).- Cotton Valley Group (Jurassic) nomenclature, Louisiana and Arkansas.- *Gulf Coast Association of Geological Societies Transactions*, vol. 14, p. 143-152.

Martinez M., Aguirre-Urreta B., Dera G., Lescano M., Omarini J., Tunik M., O'Dogherty L., Aguado R., Company M. & Bodin S. (2023).- Synchrony of carbon cycle fluctuations, volcanism and orbital forcing during the Early Cretaceous.- *Earth-Science Reviews*, vol. 239, article 104356, 41 p.

Martinez M., Deconinck J.-F., Pellenard P., Riquier L., Company M., Reboulet S. & Moiroud M. (2015).- Astrochronology of the Valanginian-Hauterivian stages (Early Cretaceous): Chronological relationships between the Paraná-Etendeka large igneous province and the Weissert and the Faraoni events.- *Global and Planetary Change*, vol. 131, p. 158-173.

Möller C., Bornemann A. & Mutterlose J. (2020).- Climate and paleoceanography controlled size variations of calcareous nannofossils during the Valanginian Weissert Event (Early Cretaceous).- *Marine Micropaleontology*, vol. 157, article 101875, 13 p.

Möller C., Mutterlose J. & Alsen P. (2015).- Integrated stratigraphy of Lower Cretaceous sediments (Ryazanian-Hauterivian) from North-East Greenland.- *Palæogeography, Palæoclimatology, Palæoecology*, vol. 437, p. 85-97.

Morales C., Gardin S., Schhnyder J., Spangenberg J., Arnaud Vanneau A., Arnaud H., Adatte T. & Föllmi K.B.F. (2013).- Berriasian and early Valanginian environmental change along a transect from the Jura Platform to the vocontian Basin.- *Sedimentology*, vol. 60, no. 1, p. 36-63.

Mucci A., Canuel R. & Zhong S. (1989).- The solubility of calcite and aragonite in sulfate-free seawater and the seeded growth kinetics and composition of the precipitates at 25°C.- *Chemical Geology*, vol. 74, nos. 3-4, p. 309-320.

Müller R.D., Dutkiewica A., Seton M. & Gaina C. (2013).- Seawater chemistry driven by supercontinent assembly, breakup, and dispersal.- *Geology*, vol. 41, no. 8, p. 907-910.

O'Brien C.L., Robinson S.A., Pancost R.D., Sinninghe Damsté J.S., Schouten S., Lunt D.J., Alsenz H., Bornemann A., Bottini C., Brassell S.C., Farnsworth A., Forster A., Huber B.T., Inglis G.N., Linnert C., Littler K., Markwick P., McAnena A., Mutterlose J., Naafs B.D.A., Püttmann W., Sluijse A., Helmond N.A.G.M. van, Vellekoop J., Wagner T., Neil E. & Wrobel N.E. (2017).- Cretaceous sea-surface temperature evolution: Constraints from TEX86 and planktonic foraminiferal oxygen isotopes.- *Earth-Science Reviews*, vol. 172, p. 224-247. DOI: 10.1016/j.earscirev.2017.07.012

Ölveczká D., Tomašových A., Reháková D., Schlögl J. & Michalík J. (2024).- Assessing temporal transition between microgranular and hyaline tests of calcareous microplankton during the Late Jurassic.- *Marine Micropaleontology*, vol. 190, article 102379, 15 p.

Percival L.M.E., Ownsworth E., Robinson S.A., Selby D., Goderis S. & Claeys P. (2023).- Valanginian climate cooling and environmental change driven by Paraná-Etendeka basalt erosion.- *Geology*, vol. 51, no. 8, p. 753-757. DOI: 10.1130/G51202.1

Pratt L.M. & Threlkeld C.N. (1984).- Stratigraphic significance of 13C/12C ratios in mid-Cretaceous rocks of the Western Interior, U.S.A. *In*: Stott D.F. & Glass D.J. (eds.), The Mesozoic of Middle North America.- *Canadian Society of Petroleum Geologists Memoir*, vol. 9, p. 305-312.

Price G.D., Főzy I. & Pálfy J. (2016).- Carbon cycle history through the Jurassic - Cretaceous boundary: A new global δ13C stack.- *Palæogeography, Palæoclimatology, Palæoecology*, vol. 451, p. 46-61.

Ray D.C., Buchem F.S.P. van, Baines G., Davies A., Gréselle B., Simmons M.D. & Robson C. (2019).- The magnitude and cause of short-term eustatic Cretaceous sea-level change: A synthesis.- *Earth-Science Reviews*, vol. 197, article 102901, 20 p.

Reháková D. & Michalík J. (1997).- Evolution and distribution of calpionellids - the most characteristic constituents of Lower Cretaceous Tethyan microplankton.- *Cretaceous Research*, vol. 18, no. 3, p. 493-504.

Remane J. (1985).- Calpionellids. *In*: Bolli H.M., Saunders J.B. & Perch Nielsen K. (eds.), Plankton stratigraphy.- Cambridge University Press, p. 555-572.

Riding J.B., Fensome R.A., Soyer-Gobillard M.-O. & Medlin L.K. (2023).- A review of the Dinoflagellates and their evolution from fossils to modern.- *Journal of Marine Science and Engineering*, vol. 11, no. 1, 34 p. DOI: 10.3390/jmse11010001

Scotese C.R. (2013).- Map Folio 29, Early Cretaceous (Hauterivian, 132.0 Ma).- DOI: 10.13140/2.1.1284.1768

Scotese C.R., Vérard C., Burgener L., Elling R.P. & Kocsis A.T. (2024).- The Cretaceous world: Plate tectonics, palaeogeography and palaeoclimate.- *GSL Special Publications*, vol. 544, p. 31-202.

Scott M. & Lindsey R. (2025).- What's the hottest Earth's ever been?- NOAA. URL: https://www.climate.gov/news-features/climate-qa/whats-hottest-earths-ever-been

Scott R.W. (1990).- Chronostratigraphy of the Cretaceous carbonate shelf, southeastern Arabia.- *GSL Special Publications*, vol. 49, p. 89-108.

Scott R.W. (2019).- Valanginian Knowles Limestone, East Texas: Biostratigraphy and potential hydrocarbon reservoir.- *Gulf Coast Association of Geological Societies Journal*, vol. 8, p. 79-88. URL: https://www.gcags.org/Journal/2019.GCAGS.Journal/2019.GCAGS.Journal.v8.06.p79-88.Scott.pdf

Scott R.W. (2022).- Tithonian-Hauterivian chronostratigraphy (latest Jurassic-Early Cretaceous), Mediterranean-Caucasian Subrealm and southern Andes: A stratigraphic experiment and Time Scale.- *Carnets Geol.*, Madrid, vol. 22, no. 13, p. 619-660. DOI: 10.2110/carnets.2022.2213

Scott R.W., Brett C.E., Fluegeman R.H., Pratt B.R. & Landing E. (2023).- North American Commission on stratigraphic Nomenclature, Report 15 - Revised articles 2, 61 and 62 of the North American stratigraphic Code to formalize chemostratigraphic units.- *Stratigraphy*, vol. 20, no. 3, p. 233-236.

Sheridan R.E. (1983).- 4. Site 534: Blake-Bahama Basin.- *Initial Reports DSDP*, vol. LXXVI, p. 141-340. DOI: 10.2973/dsdp.proc.76.1983

Śliwińska K.K., Jelby M.E., Grundvag S.-A., Nohr-Hansen H., Alsen P. & Olaussen S. (2020).- Dinocyst stratigraphy of the Valanginian-Aptian Rurikfjellet and Helvetiafjellet formations on Spitsbergen, Arctic Norway.- *Geological Magazine*, vol. 157, Special Issue 10, p. 1693-1714.

Steuber T., Löser H., Mutterlose J. & Parente M. (2023).- Biogeodynamics of Cretaceous marine carbonate production.- *Earth-Science Reviews*, vol. 238, article 104341, 23 p. DOI: 10.1016/j.earscirev.2023.104341

Steuber T., Scott R.W., Mitchell S.F. & Skelton P.W. (2016).- Part N, Revised, Volume 1, Chapter 26C: Stratigraphy and diversity dynamics of Jurassic-Cretaceous Hippuritida (Rudist Bivalves).- *Treatise Online*, no. 81, 17 p. DOI: 10.17161/to.v0i0.6474

Suan G., Schootbrugge B. van de, Adatte T., Fiebig J. & Oschmann W. (2015).- Calibrating the magnitude to the Toarcian carbon cycle perturbation.- *Paleoceanography*, vol. 30, no. 5, article PA002758, p. 495-509. DOI: 10.1002/2014PA002758

Szives O., Moreno-Bedmar J.A., Aguirre-Urreta B., Company M., Frau C., López-Horgue M., Pictet A., Ploch I., Salazar C., Barragán R., Latil J.-L., Lehmann J., Robert E. & Reboulet S. (2024).- Report on the 7th International Meeting of the IUGS Lower Cretaceous Ammonite Working Group, the Kilian Group (Warsaw, Poland, 21st August 2022): State of the art on the current Standard Ammonite Zonation of the Western Tethyan Mediterranean Province.- *Cretaceous Research*, vol. 153, article 105716, 14 p. DOI: 10.1016/j.cretres.2023.105716

THÖLE H., BORNEMANN A., HEIMHOFER U., LUPPOLD F.W., BLUMENBERG M., DOHRMANN R. & ERBACHER J. (2020).- Using high-resolution XRF analyses as a sequence stratigraphic tool in a mudstone-dominated succession (Early Cretaceous, Lower Saxony Basin, Northern Germany).- *Depositional Record*, vol. 6, no. 1, p. 236-258. DOI: 10.1002/dep2.83

TOMARU T., TAKASHIMA R., ORIHASHI Y., YAMANAKA T., ANDO H., ASAHARA Y., NISHI H., KUROYANAGI A. & OTSUBO T. (2025).- First evidence of the Lower Cretaceous WEISSERT Event in the Northwestern Panthalassa: Carbon isotope stratigraphy and U-Pb radiometric ages of the Somanakamura Group in Northeastern japan.- *Newsletters on Stratigraphy*, vol. 58, no. 2, p. 219-238. DOI: 10.1127/nos/2025/0868

TONG X., HU J., PAN Y., QIN Z., XI D., PENG P. & ALEDO T. (2024).- Terrestrial response to the Early Cretaceous WEISSERT Event: Insights from carbon isotope records of organic matter and leaf wax *n*-alkanes in an inland East Asian lake.- *Palæogeography, Palæoclimatology, Palæoecology*, vol. 656, article 112570, 9 p.

VERMEIJ G.J. (1977).- The Mesozoic marine revolution: Evidence from snails, predators and grazers.- *Paleobiology*, vol. 3, no. 3, p. 245 -258.

VÖRÖS A., FŐZY I., DULAI A. & SZIVES O. (2020).- Late Valanginian extinction and turnover of Tethyan brachiopods: A signal of the WEISSERT Event (Bakony Mountains, Hungary).- *Palæogeography, Palæoclimatology, Palæoecology*, vol. 555, article 109856, 15 p. DOI: 10.1016/j.palaeo.2020.109856

WEISSERT H., MCKENZIE J.A. & CHANNELL J.E.T. (1985).- Natural variations in the carbon cycle during the Early Cretaceous. *In*: The carbon cycle and atmospheric CO2: Natural variations Archean to the present.- *Geophysical Monograph*, vol. 32, p. 531-545.

WEISSERT H., JOACHIMSKI M. & SARNATHEIN M. (2008).- Chemostratigraphy.- *Newsletters on Stratigraphy*, vol. 42, no. 3, p. 145-179.

WIGGAN N.J., RIDING J.B, FENSOME R.A. & MATTIOLI E. (2018).- The Bajocian (Middle Jurassic): A key interval in the early Mesozoic phytoplankton radiation.- *Earth-Science Reviews*, vol. 180, p. 126-146. DOI: 10.1016/j.earscirev.2018.03.009